

Level schemes of ^{102}Pd and ^{100}Pd

W. F. Piel, Jr.,* G. Scharff-Goldhaber, and A. H. Lumpkin†

Brookhaven National Laboratory, Upton, New York 11973

Y. K. Lee and D. C. Stromswold‡

Johns Hopkins University, Baltimore, Maryland 21218

(Received 30 June 1980)

High-spin states have been populated in ^{102}Pd by $^{92}\text{Zr}(^{13}\text{C}, 3n\gamma)^{102}\text{Pd}$ with $E_{\text{lab}} = 56$ MeV and in ^{100}Pd by $^{91}\text{Zr}(^{12}\text{C}, 3n\gamma)^{100}\text{Pd}$ with $E_{\text{lab}} = 63$ MeV. We find in each nuclide a ground state band ($\Delta J = 2$) of positive parity extending to $J^\pi = 14^+$, as well as two negative parity bands ($\Delta J = 2$), one of odd spin and one of even spin. For ^{100}Pd , the present level scheme represents the first definitive study of excited states in this nuclide. For ^{102}Pd the present data include the first measurement of the γ -ray linear polarizations. The level energies are compared to the variable moment of inertia model, the interacting boson approximation model, and to the results of a quasiparticle calculation.

NUCLEAR REACTIONS, NUCLEAR STRUCTURE $^{92}\text{Zr}(^{13}\text{C}, 3n\gamma)^{102}\text{Pd}$, $E = 56$ MeV, $^{94}\text{Zr}(^{12}\text{C}, 4n\gamma)^{102}\text{Pd}$, $E = 69$ MeV, $^{91}\text{Zr}(^{12}\text{C}, 3n\gamma)^{100}\text{Pd}$, $E = 56, 63$ MeV; measured $E_\gamma, I_\gamma, \gamma(\theta), \gamma(t), \gamma(E), \gamma\text{-}\gamma$ coin, linear polarizations. $^{102}, ^{100}\text{Pd}$ deduced levels, γ branching, $J, \pi, \delta, t_{1/2}$ limits. Enriched $^{91}, ^{92}, ^{94}\text{Zr}$ targets, Ge(Li) detectors, Ge(Li) Compton polarimeter. Variable moment of inertia model, interacting boson approximation model, rotation alignment model.

INTRODUCTION

The present study of high-spin states populated in ^{102}Pd and ^{100}Pd by using heavy-ion reactions is part of a program to determine the level schemes of increasingly neutron deficient even-Pd nuclei which approach $N = 50$ neutrons from above. One goal is to establish the limits of validity of the extended variable moment of inertia (VMI) model.^{1,2} In contrast to strongly deformed even-even nuclei, for which a deviation from the VMI excitation energy predictions is often observed at a critical spin $J_c = 12$ to 16 for rare earth nuclei (backbending) and at still higher spins for some actinide nuclei, nuclei with only a slightly deformed or nearly spherical ground state might be expected to deviate at a smaller critical spin. For example, in the neutron-rich Te nuclei, a deviation is observed³ already for $J_c = 4$. At the same time, the nuclear angular velocity, as deduced from the familiar g vs ω^2 plot at which the backbend occurs, is larger for the Te nuclei than those observed in more deformed nuclei. Another goal is to attempt to understand the causes of deviations from the VMI predictions for the energy levels observed for the highest spin members of the ground state $\Delta J = 2$ cascade. We shall approach this problem by using the rotation alignment model in the context of the deformed shell model.

Our preliminary report⁴ on the ^{102}Pd and ^{100}Pd level schemes reported a "forking" of the ground

state cascade in each nucleus into two parallel even-spin positive-parity cascades. Subsequently, measurements⁵ of the γ - γ correlation ratios in ^{102}Pd showed that the lowest state in the second branch has a spin of $J = 8$ or 9 and not 10, as we had proposed. The problem was further investigated by a careful measurement of the linear polarizations of the relevant γ rays which indicated that $J^\pi = 9^-$ is the most probable assignment for this state.⁶ Also, we determined⁶ that the lowest state in the second branch in ^{100}Pd has $J^\pi = 8^-$ (rather than the 8^+ which we had previously proposed).⁴ In the case of ^{102}Pd , the erroneous spin assignment resulted from our failing to take into account the existence of a second γ -ray transition ($7^- \rightarrow 5^-$, 714.0 keV) which is unresolved from the γ -ray transition (714.9 keV) that connects the $J^\pi = 9^-$ and 8^+ levels.

For ^{100}Pd , the present work is the first definitive study of excited states in this nuclide. For ^{102}Pd , as will be shown, the level schemes which have been found by different groups⁴⁻¹⁷ are now nearly in complete agreement. In each nuclide, there is found in addition to the ground state cascade, an even-spin and an odd-spin $\Delta J = 2$ cascade, both of odd parity. As will be discussed below, the level schemes extend in a systematic way the level schemes which have previously been found^{16, 18-19} for $^{104}, ^{106}\text{Pd}$. High-spin states have also been reported²⁰⁻²⁷ in the neighboring odd-mass Pd nuclei^{99, 101, 103, 105} Pd. These states re-

veal more directly the location of the Nilsson single neutron orbitals than do the states in the even-Pd nuclei. We shall make use of this odd-A information to present calculated level energies based on the axially-symmetric rotation-alignment model both for the even-mass and for the odd-mass Pd nuclides.

The values of $R_4 = E_4/E_2$ are 2.29 and 2.13 for ^{102}Pd and ^{100}Pd , respectively, and bracket the value 2.23 for which the VMI parameter θ_0 vanishes. Such nuclei are extremely soft, i.e., even the smallest degree of rotation or "cranking" which promotes the nucleus from the $J^\pi = 0^+$ ground state to the first 2^+ state will increase the moment of inertia by a considerable amount (for nuclei with $1.82 < R_4 < 2.23$, the ground state moment of inertia vanishes according to the VMI model). The vibrational model²⁸ was first successfully applied to nuclei of this type. The development of the vibrational phonon model has recently been reviewed²⁹ by Iachello who proposed a specific form of the interacting boson approximation (IBA). Recently, Iachello, Arima, and Feshbach³⁰⁻³¹ have treated the case where only quadrupole bosons are included. This model predicted a large number of collective states of even parity, arranged in bands which are connected by enhanced $E2$ transitions. They later included octupole bosons in their model³² to describe negative

parity collective states as well. We shall present below a comparison of the latter form of the IBA to the experimental level schemes.

EXPERIMENTAL

The reactions $^{92}\text{Zr}(^{13}\text{C}, 3n\gamma)^{102}\text{Pd}$ at 56 MeV and $^{94}\text{Zr}(^{12}\text{C}, 4n\gamma)^{102}\text{Pd}$ at 69 MeV were utilized to populate high-spin states in ^{102}Pd using ions produced by the Brookhaven Tandem Van de Graaff Facility. For the former reaction we have measured, during the course of several experiments, γ -ray excitation functions, γ - γ coincidences, γ -ray angular distributions and γ -ray lifetimes by using a pulsed beam, and γ -ray linear polarization data. For the latter reaction, we have measured γ - γ coincident intensities, γ -ray angular distributions, and γ -ray excitation functions.

Figure 1 shows the γ -ray singles data obtained from $^{92}\text{Zr}(^{13}\text{C}, 3n\gamma)^{102}\text{Pd}$ at 56 MeV. The ^{92}Zr target was enriched to 95%. The data shown were obtained with the Ge(Li) detector located at eight different angles ranging from 60° to 162° with respect to the beam direction and subsequently summed. The peaks which are assigned to ^{102}Pd are labeled with their energies. We have also indicated the strongest lines from ^{101}Pd , ^{103}Pd , ^{98}Ru , ^{99}Ru , and ^{92}Zr which are simultaneously produced. In a separate experiment utilizing this reaction,

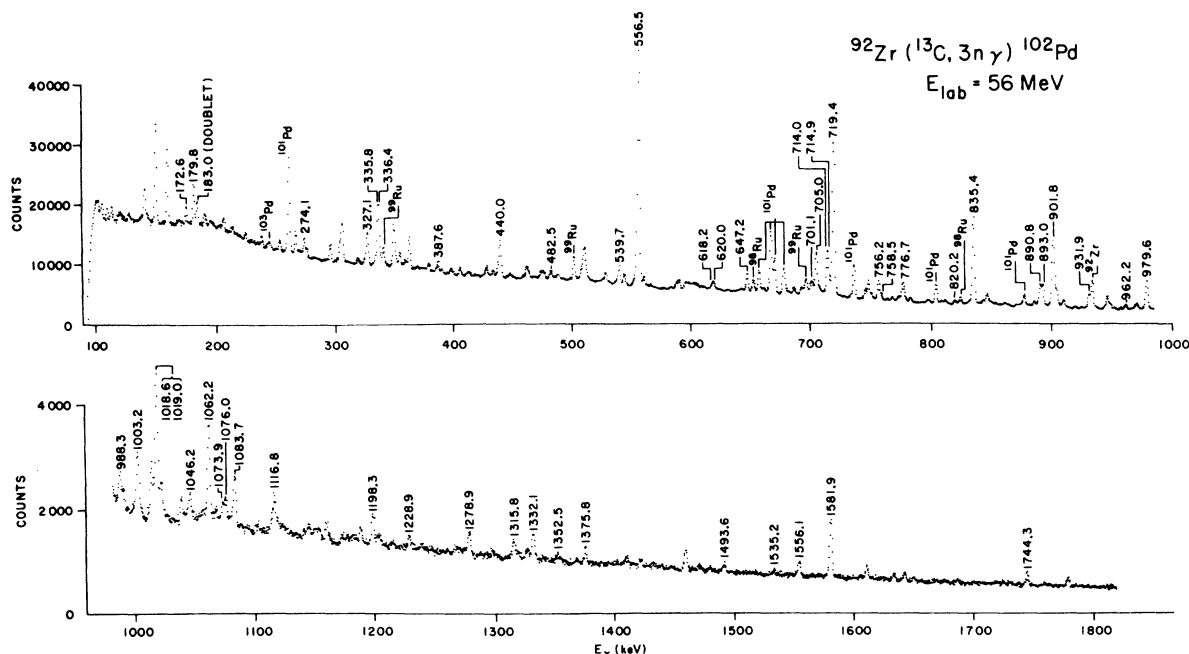


FIG. 1. A Ge(Li) γ -ray spectrum produced by ^{13}C on ^{92}Zr at 56 MeV. The transitions assigned to ^{102}Pd are labeled with their energies (in keV). Prominent transitions in ^{101}Pd , ^{103}Pd , ^{98}Ru , ^{99}Ru , and ^{92}Zr are also indicated. This spectrum is the sum of eight spectra recorded with the Ge(Li) detector located at eight distinct angles ranging from 60° to 162° with respect to the beam direction.

γ - γ coincidences ($2\tau \sim 25$ ns) were event-mode recorded on magnetic tape utilizing two 85 cm^3 Ge(Li) detectors. One detector was located at 90° and the other at 0° with respect to the ^{13}C beam direction. For aligned nuclear states, this detector arrangement yields a partial γ - γ angular correlation measurement³³ in addition to the coincident intensity information. The level scheme for ^{102}Pd which we have deduced from a careful consideration of the observed coincidences is shown in Fig. 2. Several of the levels shown are also known from previous work. Several previously known levels are populated weakly or not at all in the present work and are labeled accordingly: (a) γ rays produced by $^{99}\text{Ru}(\alpha, n\gamma)^{102}\text{Pd}$ with $E = 17$ MeV; (b) γ rays following the decay of ^{102}Ag to ^{102}Pd ; and (c) internal conversion electrons following the EC- β^+ decay of ^{102}Ag to ^{102}Pd . These levels have been included in Fig. 2 in order to show a complete picture of what is known about the level structure of ^{102}Pd . This level scheme is discussed in detail below and is compared with a previously reported level scheme obtained for ^{102}Pd

by other investigators.¹⁶ Three additional experiments were performed to aid in assigning spins and parities to the levels shown in Fig. 2. The angular distributions, the linear polarizations, and the lifetimes (the last using a pulsed beam) were measured. All of these data were acquired using the same reaction, beam energy, and ^{92}Zr target (6 mg/cm^2 , $\Delta E = 9 \text{ MeV}$) in order to simplify the analysis.

The γ -ray angular distributions were recorded using a 60 cm^3 Ge(Li) detector. The detector was situated at one of eight angles (for typically 10 min) and then, under computer control, moved to the next angle. The eight angles with respect to the beam were 60° , 75° , 90° , 105° , 120° , 135° , 150° , and 162° . The counting time at each angle was normalized to the number of γ rays with $E_\gamma > 600 \text{ keV}$ which were recorded by a Ge(Li) monitor detector placed at 90° and on the other side of the beam line. The spectra acquired from all eight angles are added and presented in Fig. 1, as mentioned above.

The γ -ray linear polarizations were measured

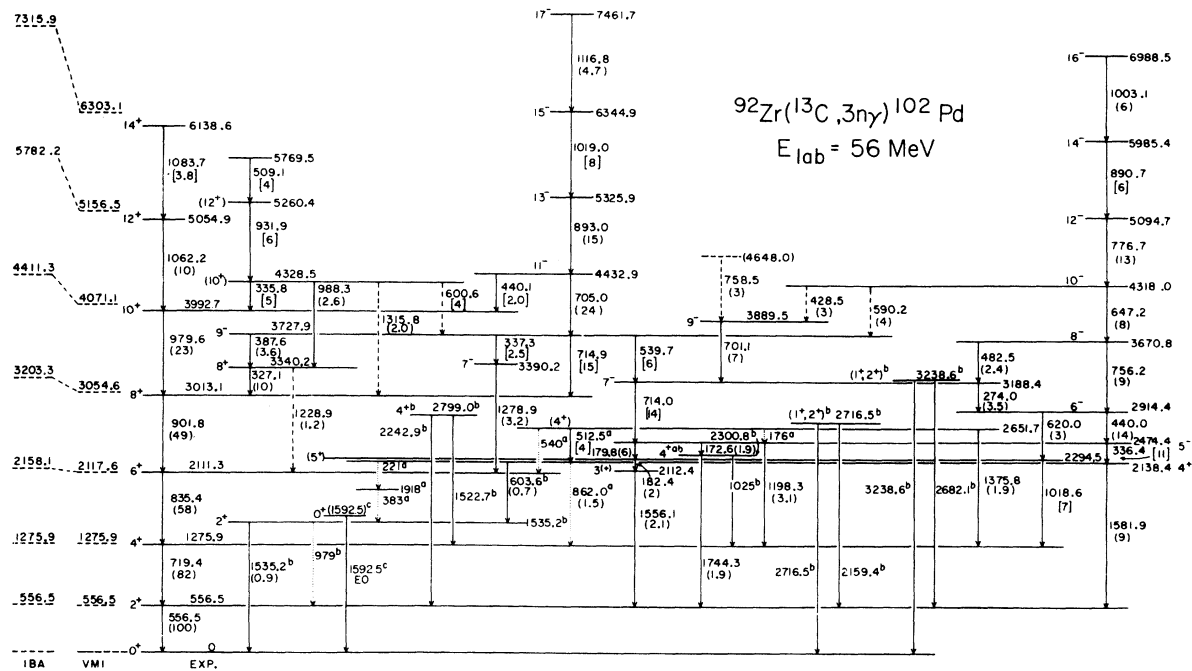


FIG. 2. The proposed level scheme of ^{102}Pd . Most of the levels are deduced from the present work. Other transitions, which have been more definitely assigned in previous studies, are also included in order to present a more complete level scheme. These are labeled: (a) γ rays produced by $^{99}\text{Ru}(\alpha, n\gamma)^{102}\text{Pd}$ with $E_{\text{lab}} = 17$ MeV; (b) γ rays following the decay of ^{102}Ag to ^{102}Pd ; and (c) internal conversion electrons following the decay of ^{102}Ag to ^{102}Pd . Also shown are the calculated ground state band energies according to the IBA and VMI models as discussed in the text. All known levels are shown except for 20 new levels of low spin between 1.6 and 3.1 MeV which have recently been found (Ref. 51) from inelastic proton scattering with $E_{\text{lab}} = 8$ MeV. The numbers in parentheses are relative transition intensities determined from singles spectra while those in brackets are determined from coincident spectra. Both types have been corrected for Ge(Li) detector efficiencies. The transitions shown by dotted vertical lines are seen more definitely in previous work. The ones drawn with dashed lines can be placed only tentatively by the present study.

using the Johns Hopkins University Ge(Li)-Ge(Li) two-crystal Compton polarimeter.^{25,34,35} The polarimeter was located at 90° and data were acquired with the crystals in two different positions. One position was with the axis connecting the two crystals in the plane defined by the ^{13}C beam and the detected γ ray, and the other position was with the axis perpendicular to this plane. We event-mode recorded coincidences (~ 80 Hz) between the two polarimeter crystals. The counting time for each of the two polarimeter positions was normalized to the number of singles γ -ray events from a fixed Ge(Li) detector with $E_\gamma > 600$ keV. The results of these measurements are discussed below.

For the nuclide ^{100}Pd , Fig. 3 shows the γ -ray singles data obtained from $^{91}\text{Zr}(^{12}\text{C}, 3n\gamma)^{100}\text{Pd}$ with $E_{\text{lab}} = 63$ MeV. As in the case of ^{102}Pd , the γ -ray spectrum shown was obtained by adding the spectra recorded at eight distinct angles. The γ - γ coincidences, γ -ray linear polarizations, and γ -ray lifetimes were also recorded in separate ex-

periments for this reaction as was described above for ^{102}Pd . In addition, the angular distributions of γ rays produced by the reaction $^{91}\text{Zr}(^{12}\text{C}, 3n\gamma)^{100}\text{Pd}$, with $E_{\text{lab}} = 56$ MeV, were measured. The level scheme, which is displayed in Fig. 4, was deduced from the γ -ray coincidences and displays all of the excited states of ^{100}Pd which can be inferred. We have included two additional states of ^{100}Pd in Fig. 4 which are now known³⁶ from the $^{98}\text{Ru}(^{16}\text{O}, ^{12}\text{C})^{100}\text{Pd}$ reaction with $E_{\text{lab}} = 70$ MeV and $\theta_{\text{lab}} = 40^\circ$. The ^{12}C ions were detected by a 70 cm proportional counter located in the focal plane of the Brookhaven QDDD magnet facility.

RESULTS

A. ^{102}Pd

The numerical results for ^{102}Pd are summarized in Table I. The first column lists the transition energies, and the second column lists the relative γ -ray intensities which have been corrected for the detector efficiency and for the transmission of a

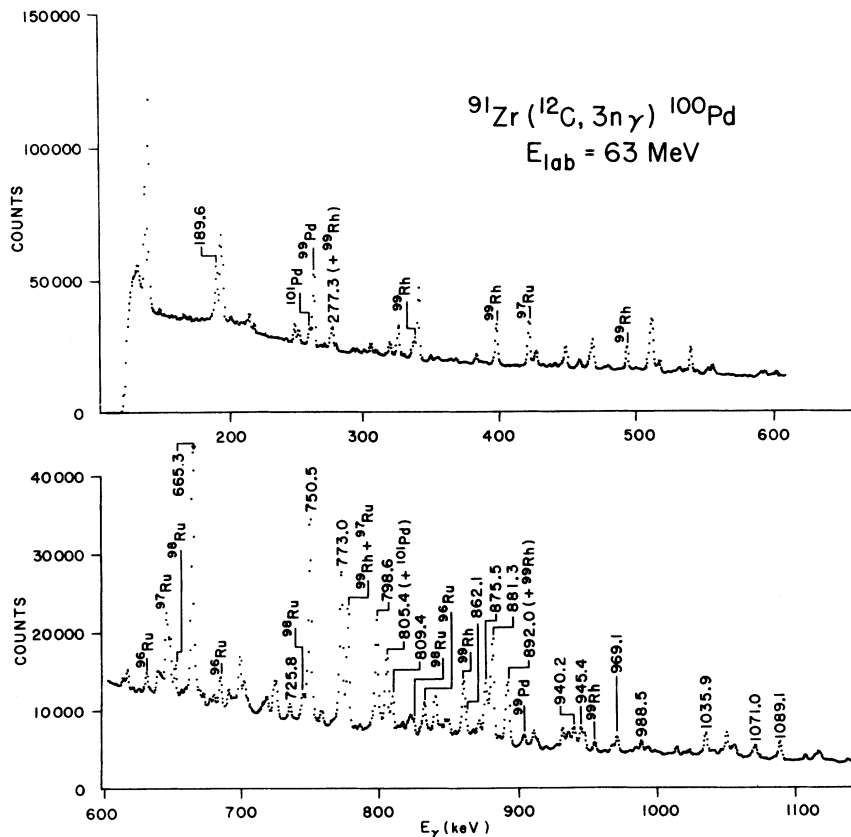


FIG. 3. A Ge(Li) γ -ray spectrum produced by ^{12}C on ^{91}Zr with $E_{\text{lab}} = 63$ MeV. The transitions assigned to ^{100}Pd are labeled with their energies (in keV). Prominent transitions in ^{99}Pd , ^{101}Pd , ^{99}Rh , ^{96}Ru , ^{97}Ru , and ^{98}Ru are also labeled. This spectrum is the sum of eight spectra recorded with the Ge(Li) detector located at eight distinct angles ranging from 60° to 164° with respect to the beam direction.

TABLE I. Transitions in ^{102}Pd produced by 56 MeV $^{13}\text{C} + ^{92}\text{Zr}$. The correlation ratio R is defined by Eq. (2) and M is the number of coincident stretched $E2$ transitions used to determine R .

Transition energy (keV)	Relative intensity	A_2/A_0	A_4/A_0	R	M	Linear polarization	Assignment
172.6 ± 0.7	1.93 ± 0.09	-0.29 ± 0.09	+0.05 ± 0.13			-0.38 ± 0.43	$5^- \rightarrow 4_2^+$
179.8 ± 0.7	6.37 ± 0.14	+0.41 ± 0.06	+0.05 ± 0.08			-0.45 ± 0.24	$5^- \rightarrow (5^+)$
182.4 ± 0.7 } 183.0 ± 0.7 }	3.55 ± 0.13	-0.09 ± 0.07	+0.19 ± 0.11			-0.16 ± 0.20	One of these is $(5^+) \rightarrow 3^{(+)}$. The other is probably in ^{102}Pd
274.04 ± 0.22	3.48 ± 0.14	+0.051 ± 0.050	-0.025 ± 0.075	1.16 ± 0.47	2	-0.26 ± 0.10	$7^- \rightarrow 6^-$ $\delta = +0.20 \pm 0.07$
327.14 ± 0.15	10.32 ± 0.28	+0.201 ± 0.040	+0.045 ± 0.059	0.98 ± 0.10	5	0.41 ± 0.10	$8_2^+ \rightarrow 8^+$ $\delta = -0.27 \pm 0.13$
335.8 ± 0.5 } 336.41 ± 0.22 }	18.60 ± 0.59	-0.042 ± 0.021	-0.040 ± 0.031	0.67 ± 0.18	2 } 4 }	0.306 ± 0.028	$(10_2^+) \rightarrow 10^+$
337.3	2.5						$9^- \rightarrow 7_2^-$
387.57 ± 0.31	3.55 ± 0.28	-0.50 ± 0.13	+0.13 ± 0.19	2.70 ± 0.75	5	0.35 ± 0.15	$9^- \rightarrow 8_2^+$
428.48 ± 0.36	3.41 ± 0.28	-0.26 ± 0.10	-0.09 ± 0.15			-0.30 ± 0.12	$(10^- \rightarrow 9_2^-)$ $\delta = -0.05 \pm 0.07$
440.00 ± 0.18	13.6 ± 0.8	+0.247 ± 0.029	+0.018 ± 0.042	0.94 ± 0.10	5	-0.492 ± 0.050	$6^- \rightarrow 5^-$ $\delta = +0.40 \pm 0.09$
440.1	2						$11^- \rightarrow 10^+$
482.51 ± 0.10	2.45 ± 0.19	+0.40 ± 0.11	+0.17 ± 0.16	0.84 ± 0.31	2	-0.46 ± 0.20	$8^- \rightarrow 7^-$ $\delta = +1.5 \pm 0.5$
509.1 ± 0.9 } 512.5 ± 0.9 }	<17			1.37 ± 0.24	5		$\rightarrow (12_2^+)$
539.74 ± 0.15	7.84 ± 0.26	+0.248 ± 0.047	-0.054 ± 0.069	0.93 ± 0.29	2		$(4_2^+ \rightarrow 4_2^+)$
556.49 ± 0.15	$\equiv 113.0^a \pm 2.0$	+0.305 ± 0.010	-0.092 ± 0.010	1.01 ± 0.23	3	0.35 ± 0.07	$9^- \rightarrow 7^-$
590.22 ± 0.30	4.42 ± 0.33	0.00 ± 0.09	-0.12 ± 0.13			0.454 ± 0.014	$2^+ \rightarrow 0^+$ $(10^- \rightarrow 9^-)$ $\delta = +0.14 \pm 0.09$
600.6 ± 0.7	3.8 ± 0.7			2.7 ± 1.0	4		$(10_2^+ \rightarrow 9^-)$
603.56 ± 0.45	0.71 ± 0.22	-0.18 ± 0.12	+0.03 ± 0.16				$4_2^+ \rightarrow 2_2^+$
618.2 ± 0.5 } 620.0 ± 0.5 }	5.39 ± 0.20	-0.04 ± 0.12	+0.15 ± 0.17			0.45 ± 0.15	Possibly in ^{102}Pd
647.17 ± 0.20	7.67 ± 0.25	+0.315 ± 0.055	-0.156 ± 0.080	1.07 ± 0.27	3	0.78 ± 0.11	$6^- \rightarrow (5^+)$
701.12 ± 0.25	6.62 ± 0.48	+0.268 ± 0.035	-0.082 ± 0.051			0.76 ± 0.11	$10^- \rightarrow 8^-$
704.96 ± 0.18	23.67 ± 0.46	+0.292 ± 0.022	-0.110 ± 0.030	1.16 ± 0.07	4	0.497 ± 0.036	$9_2^- \rightarrow 7^-$ $11^- \rightarrow 9^-$
714.00 ± 0.40 } 714.88 ± 0.40 }	31.3 ^b ± 1.0	+0.20 ± 0.03	-0.09 ± 0.05	2.52 ± 0.29	2	0.379 ± 0.024	$7^- \rightarrow 5^-$ $9^- \rightarrow 8^+$
719.37 ± 0.16	92.3 ^c ± 0.9	+0.269 ± 0.010	-0.069 ± 0.012	1.048 ± 0.045	1	0.431 ± 0.024	$4^+ \rightarrow 2^+$
756.21 ± 0.25 } 758.5 ± 0.4 }	12.2 ± 0.7	+0.338 ± 0.043	-0.076 ± 0.063	1.39 ± 0.20	3	0.54 ± 0.13	$8^- \rightarrow 6^-$ $(\leftarrow 9_2^-)$
776.70 ± 0.25	13.30 ± 0.42	+0.270 ± 0.028	-0.088 ± 0.040	1.08 ± 0.20	2	0.59 ± 0.07	$12^- \rightarrow 10^-$
812.23 ± 0.40	2.86 ± 0.19						Probably occurs in ^{102}Pd
820.15 ± 0.35	2.69 ± 0.27	+0.28 ± 0.18	+0.06 ± 0.26			-0.24 ± 0.31	Probably occurs in ^{102}Pd
835.42 ± 0.12	57.9 ± 0.8	+0.289 ± 0.012	-0.052 ± 0.018	1.047 ± 0.038	2	0.513 ± 0.056	$6^+ \rightarrow 4^+$
862.05 ± 0.30	1.49 ± 0.28	-0.04 ± 0.13	+0.01 ± 0.18			0.34 ± 0.37	$(4_2^+ \rightarrow 4^+)$
890.75 ± 0.25	14.85 ± 0.33	+0.361 ± 0.054	-0.108 ± 0.080	0.68 ± 0.14	3	0.60 ± 0.07	$14^- \rightarrow 12^-$
893.05 ± 0.25	15.21 ± 0.32	+0.333 ± 0.042	-0.067 ± 0.062	0.92 ± 0.09	3	0.512 ± 0.049	$13^- \rightarrow 11^-$
901.78 ± 0.15	49.87 ^d ± 0.41	+0.271 ± 0.014	-0.045 ± 0.020	0.983 ± 0.034	3	0.52 ± 0.09	$8^+ \rightarrow 6^+$
931.87 ± 0.25	10.56 ± 0.29	+0.289 ± 0.049	-0.087 ± 0.071	0.76 ± 0.14	5	0.29 ± 0.17	$(12_2^+ \rightarrow 10_2^+)$
962.16 ± 0.40	4.17 ± 0.42	+0.05 ± 0.12	-0.14 ± 0.17			0.20 ± 0.32	^{102}Pd
979.65 ± 0.25	23.41 ± 0.28	+0.251 ± 0.022	-0.052 ± 0.032	1.011 ± 0.052	4	0.638 ± 0.059	$10^+ \rightarrow 8^+$
988.30 ± 0.30	2.60 ± 0.17	+0.02 ± 0.11	+0.04 ± 0.16			0.68 ± 0.24	$(10_2^+) \rightarrow 8_2^+$
1003.15 ± 0.30	5.78 ± 0.20	+0.25 ± 0.07	-0.21 ± 0.10	2.13 ± 0.46	4	0.64 ± 0.18	$16^- \rightarrow 14^-$
1018.6 ± 0.4 } 1019.0 ± 0.4 }	15.18 ± 0.24	+0.236 ± 0.029	-0.048 ± 0.042	1.09 ± 0.28	2	0.49 ± 0.08	$(5^+) \rightarrow 4^+$
1046.25 ± 0.40	2.45 ± 0.20	+0.19 ± 0.12	-0.19 ± 0.17			0.48 ± 0.26	$15^- \rightarrow 13^-$ ^{102}Pd

TABLE I. (Continued).

Transition energy (keV)	Relative intensity	A_2/A_0	A_4/A_0	R	M	Linear polarization	Assignment
1062.25 ± 0.18	9.58 ± 0.20	+0.240 ± 0.051	-0.032 ± 0.075			0.58 ± 0.13	12 ⁺ → 10 ⁺
1073.92 ± 0.40	1.74 ± 0.20	0.60 ± 0.16	+0.07 ± 0.22			0.43 ± 0.40	Possibly in ^{102}Pd
1076.04 ± 0.35	2.34 ± 0.20	0.17 ± 0.11	-0.22 ± 0.16			0.24 ± 0.43	Possibly in ^{102}Pd
1083.71 ± 0.32	5.37 ^e ± 0.23	+0.226 ± 0.066	-0.141 ± 0.098			0.39 ± 0.25	14 ⁺ → 12 ⁺
1116.80 ± 0.40	4.69 ± 0.28	+0.34 ± 0.10	-0.04 ± 0.14			0.66 ± 0.28	17 ⁻ → 15 ⁻
1198.29 ± 0.18	3.10 ± 0.16	-0.23 ± 0.11	-0.05 ± 0.16			-0.28 ± 0.29	5 ⁻ → 4 ⁺
1228.93 ± 0.35	1.21 ± 0.19					0.39 ± 0.61	(8 ₂ ⁺ → 6 ⁺)
1278.91 ± 0.40	3.21 ± 0.17	-0.25 ± 0.10	-0.12 ± 0.15			0.45 ± 0.28	7 ₂ ⁻ → 6 ⁺
1315.8 ± 0.7	2.01 ± 0.13	+0.05 ± 0.17	+0.00 ± 0.24				(10 ₂ ⁺ → 8 ⁺)
1332.1 ± 0.7	3.84 ± 0.23	-0.05 ± 0.09	-0.09 ± 0.14			0.47 ± 0.47	Probably occurs in ^{102}Pd
1352.5 ± 0.8	1.19 ± 0.23						Possibly occurs in ^{102}Pd
1375.81 ± 0.40	1.87 ± 0.18	+0.43 ± 0.15	+0.12 ± 0.22			0.48 ± 0.52	(4 ₁ ⁺) → 4 ⁺ δ = +0.61 ± 0.63
1493.6 ± 0.7	1.33 ± 0.13	-0.28 ± 0.20	+0.04 ± 0.29				Possibly in ^{102}Pd
1535.19 ± 0.50	0.88 ± 0.09						2 ₂ ⁺ → 0 ⁺
1556.10 ± 0.50	2.33 ± 0.13	-0.07 ± 0.13	+0.16 ± 0.19			-0.21 ± 0.51	3 ⁽⁺⁾ → 2 ⁺
1581.94 ± 0.20	9.43 ± 0.22	+0.281 ± 0.045	-0.038 ± 0.065			0.23 ± 0.23	4 ₂ ⁺ → 2 ⁺
1744.34 ± 0.40	1.94 ± 0.18	+0.26 ± 0.16	+0.19 ± 0.24				4 ₃ ⁺ → 2 ⁺

^a 13% of this intensity is an unresolved transition in ^{101}Pd .

^b 2.4% of this intensity is an unresolved transition in ^{103}Pd .

^c 1.4% of this intensity is an unresolved transition in ^{103}Pd and 9.0% is due to a transition in ^{99}Ru .

^d 0.7% of this intensity is due to two unresolved transitions in ^{101}Pd .

^e 1.6% of this intensity is due to an unresolved transition in ^{101}Pd .

copper absorber which was used to attenuate the Zr target x rays. These intensities are obtained from best fits to the summed angular distribution data except for the cases of overlapping γ -ray peaks. In each of these special cases, the intensity is determined from the coincident intensities. An additional check that a particular peak is completely resolved from other peaks is provided by requiring that the relative singles intensity and coincident intensity agree, after correcting for the angular correlation. The third and fourth columns of Table I list the A_2/A_0 and A_4/A_0 values obtained from a best fit to the angular distribution data. These values are obtained by fitting the expression

$$W(\theta) = A_0 + A_2 P_2(\cos\theta) + A_4 P_4(\cos\theta) \quad (1)$$

to the background subtracted peak areas at all eight angles, where P_2 and P_4 are Legendre polynomials, and A_0 , A_2 , and A_4 are the adjustable parameters. The values of A_2/A_0 and A_4/A_0 listed in the third and fourth columns in Table I have been corrected slightly for the solid angle subtended by the Ge(Li) detector.

To be concise, we shall not tabulate all possible coincident intensities which led to the level scheme shown in Fig. 2. We shall, however, ex-

PLICITLY point to the controversial cases involving the weakest transitions. Moreover, it is useful to tabulate the correlation ratio R which is presented in the fifth column of Table I. The correlation ratio R is defined as follows. Let γ_1 and γ_2 be two coincident γ -ray transitions. Let I_N be the coincident rate of γ_1 striking detector 2 (at 90°) and γ_2 simultaneously striking detector 1 (at 0°). Let I_D be the coincident rate of γ_1 striking detector 1 and γ_2 simultaneously striking detector 2. We define R for γ_1 (where γ_1 precedes γ_2) by

$$R(\gamma_1) = I_N/I_D. \quad (2)$$

The ratio R is referred to as the directional correlation ratio³³ from an oriented state (DCO ratio). It turns out that R is unchanged by any unobserved stretched transitions between γ_1 and γ_2 as long as the magnetic substate populations of the nuclear spin are not disturbed by the nuclear environment. In this paper, we shall let γ_1 be the γ ray of interest and γ_2 will always be a transition known to be a coincident stretched $E2$ transition (usually a member of the ground state cascade). For example, consider the entry 0.98 ± 0.10 listed in the fifth column of Table I for $\gamma_{327.1}$. For this transition, there are four coincident $E2$ transitions in the ground state cascade. Each of the four stret-

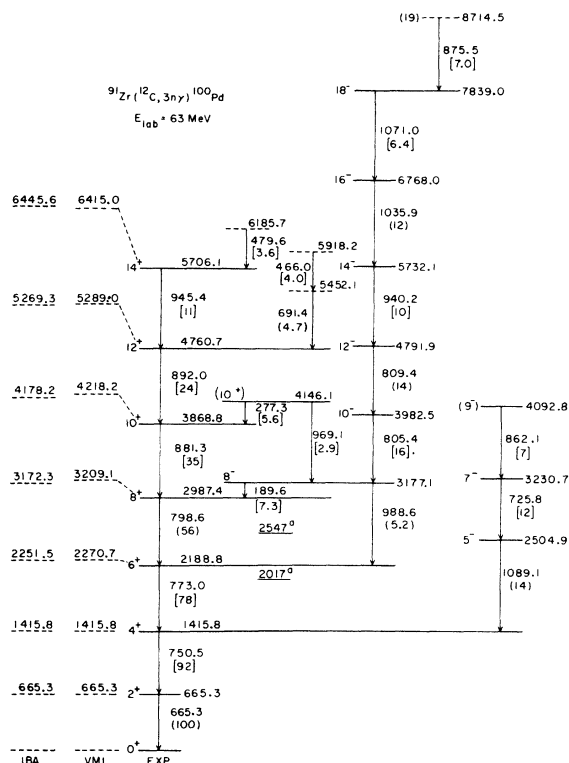


FIG. 4. The proposed level scheme of ^{100}Pd . Also shown are the calculated ground state band energies according to the IBA and VMI models as discussed in the text. The two levels labeled with an "a" have been found (Ref. 36) using the $^{96}\text{Ru}(^{16}\text{O}, ^{12}\text{C})^{100}\text{Pd}$ reaction. The numbers in parentheses are relative transition intensities determined from singles spectra while those in brackets are determined from coincident spectra. Both types have been corrected for Ge(Li) detector efficiencies. The dashed levels can be inferred only tentatively from the data.

ched $E2$'s yields a value for R using Eq. (2). The theory³³ tells us that all four values of R should be the same. Therefore, to gain greater accuracy, we average the four experimental values for the ratio R for $\gamma_{327.1}$. In this case, there is another intense coincident stretched $E2$, namely $\gamma_{705.0}$, so that five stretched $E2$'s were used to obtain the average value of $R = 0.98 \pm 0.10$. (In doing this, we ignore any difference in the alignment of the 3340.2- and 4432.9-keV levels.) Therefore, we have entered a "5" in the sixth column of Table I to indicate that five stretched $E2$ transitions are used to evaluate R for $\gamma_{327.1}$. If $\gamma_{327.1}$ were a pure-stretched quadrupole ($E2$ or $M2$) transition, then the anticipated value would be $R = 1$. However, if $\gamma_{327.1}$ were a pure-stretched dipole transition, the value (depending on the alignment of the level at 3340.2 keV in Fig. 2) would be about $R = 2$. In

practice, a continuous range of values for R is possible for various values of the quadrupole-dipole mixing ratio for the transition of interest and for various values of the spin and alignment of the γ -ray emitting state. We find it convenient to use, instead of R , the quantity $(R - 1)/(R + 1)$ and shall shortly discuss several plots of this quantity which can take on any value from -1 to $+1$ (for point detectors).

This technique has previously been used⁵ to show that $\gamma_{714.9}$ is not a stretched quadrupole transition (in which case $R = 1$) as we had previously proposed.⁴ From Table I, the average value of R for $\gamma_{714.9}$ when taken in coincidence with $\gamma_{835.4}$ and $\gamma_{901.8}$ is $R = 2.52 \pm 0.29$. Thus the spin of the level at 3727.9 keV in ^{102}Pd can only be $J = 7, 8, \text{ or } 9$. We shall discuss this level in more detail below.

The seventh column of Table I lists the results of the linear polarization measurements. We measured the two counting rates $I(0^\circ)$ and $I(90^\circ)$ with the polarimeter axis in the reaction plane and perpendicular to the reaction plane, respectively. The linear polarization P is then defined by

$$P = \frac{I(90^\circ) - I(0^\circ)}{I(90^\circ) + I(0^\circ)} \frac{1}{Q}, \quad (3)$$

where Q denotes the sensitivity of the polarimeter to the linear polarization. The quantity Q decreases smoothly from $Q \cong 0.5$ for $E_\gamma = 250$ keV to $Q \cong 0.2$ for $E_\gamma = 1500$ keV. The calibration of Q is accomplished by recording γ -ray transitions of known multipolarity which are emitted by nuclear states whose alignment has been determined by measuring γ -ray angular distributions. A calibration of Q is displayed in Fig. 1 of Ref. 19. The linear polarization P can range, in principle, from $+1$, e.g., for stretched pure-electric transitions, to -1 , e.g., for stretched pure-magnetic transitions. The linear polarization is usually larger in magnitude whenever the emitting nuclear state is more aligned as is also true for the three quantities A_2/A_0 , A_4/A_0 , and $(R - 1)/(R + 1)$. For an isotropic initial nuclear state, the four quantities P , A_2/A_0 , A_4/A_0 , and $(R - 1)/(R + 1)$ vanish for subsequent γ rays.

We now discuss the detailed findings first for the level scheme of ^{102}Pd shown in Fig. 2. The set of seven transitions which successively depopulate the level at 6138.6 keV form a $\Delta J = 2(E2)$ cascade populating the $J^\pi = 0^+$ ^{102}Pd ground state. The A_2/A_0 , A_4/A_0 , R , and P values support this interpretation. We do not list values of R for the highest energy transitions in Table I, as these are thought to be unreliable due to an experimental difficulty with the electronics. The set of four transitions which successively depopulate the level at 7461.7 keV, namely $\gamma_{1116.8}$, $\gamma_{1019.0}$, $\gamma_{893.0}$, and

$\gamma_{705.0}$, are also stretched $E2$ transitions. To determine the J^π values for levels in this latter cascade, we now deduce the J^π value for the 3727.9-keV level, which is depopulated by $\gamma_{714.9}$ to the $J^\pi = 8^+$ member of the ^{102}Pd ground state cascade, by $\gamma_{387.6}$ to the level at 3340.2 keV and by $\gamma_{539.7}$ to the level at 3188.4 keV. The 3340.2-keV level is depopulated by $\gamma_{327.1}$ to the $J^\pi = 8^+$ member of the ground state cascade as shown in Fig. 2.

In Fig. 5, we plot experimental values of A_4/A_0 vs A_2/A_0 for $\gamma_{387.6}$ and $\gamma_{327.1}$ in ^{102}Pd which were obtained by fitting Eq. (1) to the angular distribution data. We also display the quantity $(R-1)/(R+1)$, where R is given by Eq. (2), and the linear polarization P . Because the 3340.2-keV level is depopulated by $\gamma_{327.1}$ and $\gamma_{1228.9}$, which populate the $J^\pi = 8^+$ and 6^+ levels, respectively, this level can only have a spin of $J=7$ or 8. A spin of $J=9$ is ruled out by our pulsed-beam lifetime measurements since, in that case, $\gamma_{1228.9}$ would have had a measurable lifetime—which is not observed. A spin of $J=6$ is also ruled out since, in that case, $\gamma_{327.1}$ would be expected³⁷ to have a small negative (≈ -0.046) value of A_4/A_0 which is characteristic of a stretched quadrupole transition from an aligned state. However, both Tables I and II reveal a small positive experimental value of A_4/A_0 for $\gamma_{327.1}$. An examination of the data for $\gamma_{327.1}$ shown in Fig. 6 shows that J^π for the 3340.2-

keV level is either 8^+ or 7^- (the curve for $J^\pi = 7^-$ is very similar to the curve shown for $J^\pi = 9^-$ —with the sign of the mixing ratio reversed). Each curve represents the locus of possible locations of a datum for all possible (real) values of the quadrupole-dipole mixing ratio δ . A datum, then, is expected to lie *on* the appropriate curve and not merely somewhere in the interior. The choice of $J^\pi = 8^+$ is strongly favored for two reasons: (1) the choice of $J^\pi = 7^-$ suggests that $\gamma_{1228.9}$ would be expected to be more intense than $\gamma_{327.1}$; (2) the choice of $J^\pi = 7^-$ would cause contradictions with respect to spin assignments for the connected levels at 3188.4, 2914.4, and 2474.4 keV as we shall discuss below. Therefore, we propose that $J^\pi = 8^+$ for the 3340.2-keV level in ^{102}Pd . Proceeding from this choice, the 3727.9-keV level can only have spin $J=7, 8,$ or 9 since $\gamma_{714.9}$ does not have the DCO ratio R appropriate to a stretched quadrupole transition ($R=1$), as has also been shown previously.⁵ Moreover, an appreciable octupole admixture is ruled out by the measured upper limit for the half-life of 5 ns. A spin of 7 for the 3727.9-keV level is not suggested both because a transition of 1616.6 keV to the $J^\pi = 6^+$ member of the ^{102}Pd ground state cascade is not observed and because contradictions arise with respect to spin assignments for the connected levels at 3188.4, 2914.4, and 2474.4 keV. In the

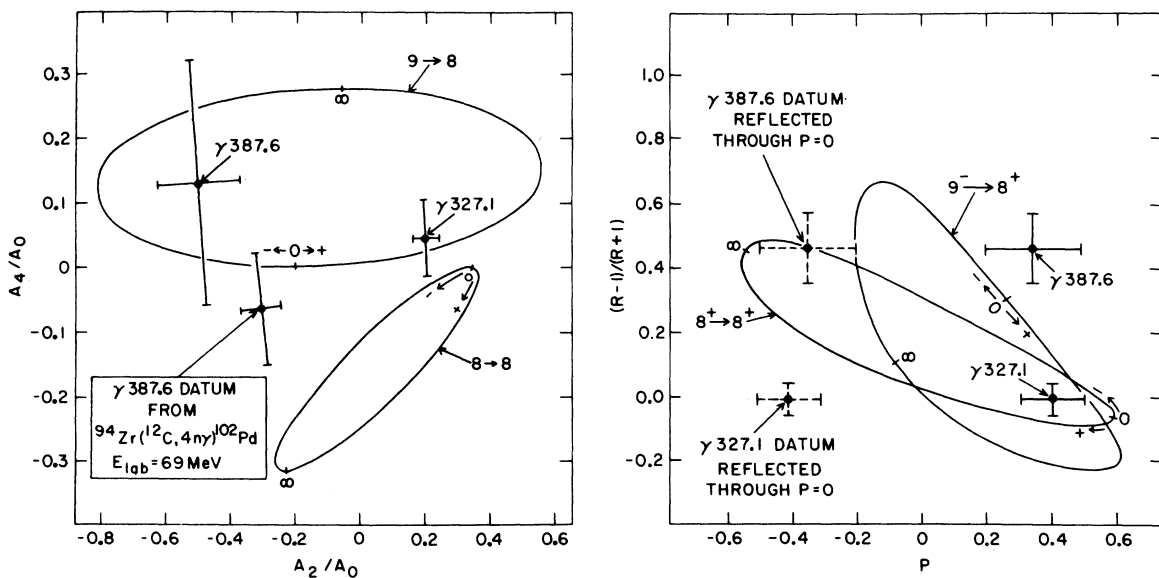


FIG. 5. The possible nuclear spin changes associated with the 387.6- and 327.1-keV transitions in ^{102}Pd . These transitions are produced by $^{92}\text{Zr}(^{13}\text{C}, 3n\gamma)$ with $E_{\text{lab}} = 56 \text{ MeV}$. The curves are calculated by assuming a Gaussian magnetic substate population (Ref. 37) of nuclear spins with the alignment coefficients: $\alpha_2 = 0.67$, $\alpha_4 = 0.50$, and $\alpha_6 = 0.10$. Also shown is a datum obtained from the $^{94}\text{Zr}(^{12}\text{C}, 4n\gamma)^{102}\text{Pd}$ reaction with $E_{\text{lab}} = 69 \text{ MeV}$. Along each closed curve, the quadrupole-dipole mixing ratio varies from 0 to $+\infty$ and from 0 to $-\infty$. The spin assignments which follow from these data are discussed in the text.

TABLE II. Transitions in ^{102}Pd produced by 69 MeV $^{12}\text{C} + ^{94}\text{Zr}$. The intensities have been corrected for the Ge(Li) detector efficiency and the A_2/A_0 and A_4/A_0 values have been slightly corrected for the finite solid angle of the detector.

Transition energy (keV)	Relative intensity	A_2/A_0	A_4/A_0
172.6	3.43 ± 0.14	-0.250 ± 0.045	0.061 ± 0.064
179.8	6.11 ± 0.61	0.304 ± 0.015	0.045 ± 0.021
182.4 } 183.0 }	3.93 ± 0.40	-0.239 ± 0.026	-0.005 ± 0.036
274.04	3.08 ± 0.20	0.130 ± 0.030	0.034 ± 0.043
327.14	9.35 ± 0.31	0.276 ± 0.022	0.020 ± 0.030
335.8 } 336.41 } 338.2 }	20 ± 2^a	-0.071 ± 0.012	0.015 ± 0.016
387.57	2.71 ± 0.19	0.160 ± 0.041	-0.079 ± 0.059
428.48	3.41 ± 0.16	-0.304 ± 0.062	-0.064 ± 0.088
440.00 } 440.1 }	3.41 ± 0.16	-0.39 ± 0.09	0.06 ± 0.12
482.51	11.80 ± 0.57	0.349 ± 0.030	0.040 ± 0.042
509.1 } 512.5 }	2.46 ± 0.29	0.63 ± 0.06	0.16 ± 0.08
526	6 ± 2^a	0.03 ± 0.07	-0.05 ± 0.10
539.74	5.5 ± 1.1^a	-0.34 ± 0.08	0.05 ± 0.11
556.49	6.7 ± 1.3^a	0.238 ± 0.011	-0.040 ± 0.015
590.22	$\cong 105.0 \pm 1.0^b$	0.310 ± 0.010	-0.069 ± 0.010
600.6	3.42 ± 0.24	-0.03 ± 0.07	0.00 ± 0.10
603.56	1.40 ± 0.13		
618.2	2.6 ± 0.4	-0.008 ± 0.044	-0.100 ± 0.063
620.0	2.7 ± 0.4	0.230 ± 0.037	-0.104 ± 0.052
647.17	8.02 ± 0.33	0.339 ± 0.028	-0.124 ± 0.035
701.12	6.1 ± 1.5^a	0.239 ± 0.036	-0.059 ± 0.051
704.96	16.68 ± 0.49	0.345 ± 0.012	-0.093 ± 0.016
714.00 } 714.88 }	19 ± 2^a	0.231 ± 0.010	-0.073 ± 0.013
719.37	82 ± 3^c	0.270 ± 0.010	-0.060 ± 0.010
756.21 } 758.5 }	11.15 ± 0.53	0.298 ± 0.020	-0.091 ± 0.029
776.70	8.8 ± 1.3^c	0.390 ± 0.030	-0.087 ± 0.042
812.23	2.1 ± 0.4	$+0.02 \pm 0.08$	-0.01 ± 0.11
820.15	2.11 ± 0.22	0.41 ± 0.11	-0.23 ± 0.15
835.42	56.2 ± 0.8	0.316 ± 0.010	-0.085 ± 0.010
862.05	2.53 ± 0.38	-0.05 ± 0.09	-0.10 ± 0.12
890.75 } 893.05 }	18 ± 3^c	0.42 ± 0.06	-0.04 ± 0.09
901.78	44.8 ± 1.0	0.260 ± 0.022	-0.090 ± 0.032
931.87	5 ± 2^c	0.332 ± 0.011	-0.083 ± 0.016
962.16	2.06 ± 0.17	0.325 ± 0.018	-0.083 ± 0.025
979.65	2.06 ± 0.17	0.28 ± 0.08	0.18 ± 0.11
988.30	18.17 ± 0.58	0.296 ± 0.011	-0.056 ± 0.015
1003.15	4.3 ± 0.7	0.06 ± 0.06^a	-0.03 ± 0.08^a
1018.6 } 1019.0 }	6.41 ± 0.18	0.350 ± 0.051	-0.007 ± 0.072
1046.25	15.2 ± 1.6^c	0.31 ± 0.07	-0.01 ± 0.10
1062.25	2.57 ± 0.17	0.21 ± 0.07	0.00 ± 0.10
1073.92	9.54 ± 0.13	0.326 ± 0.021	-0.063 ± 0.030
1076.04	2.64 ± 0.26	0.05 ± 0.06	-0.02 ± 0.09
1083.71	4.46 ± 0.20	0.161 ± 0.052	-0.051 ± 0.074
1116.80	4.2 ± 1.2^c	0.37 ± 0.08	-0.11 ± 0.11
1198.29	3.19 ± 0.15	-0.23 ± 0.05	-0.04 ± 0.07
1228.93	1.70 ± 0.09	0.14 ± 0.06	0.05 ± 0.09
1278.91	3.22 ± 0.15	-0.22 ± 0.05	0.08 ± 0.07
1315.8	1.10 ± 0.08	0.59 ± 0.12	-0.07 ± 0.17

TABLE II. (Continued).

Transition energy (keV)	Relative intensity	A_2/A_0	A_4/A_0
1332.1	6.1 ± 1.3^c	0.19 ± 0.07	-0.24 ± 0.10
1352.5	1.16 ± 0.12	0.29 ± 0.16	0.06 ± 0.22
1375.81	1.99 ± 0.08	0.28 ± 0.08	0.08 ± 0.11
1493.6	1.78 ± 0.08	-0.49 ± 0.09	-0.05 ± 0.12
1535.19	0.80 ± 0.08	0.11 ± 0.21	-0.08 ± 0.30
1556.10	2.51 ± 0.10	0.17 ± 0.06	0.14 ± 0.09
1581.94	8.25 ± 0.55	0.336 ± 0.020	-0.125 ± 0.027
1744.34			

^a This transition is unresolved from other transitions. The intensity is deduced from coincident data.

^b 5% of this intensity is due to a transition in ^{104}Pd .

^c Perturbed by an unresolved transition in ^{108}Pd .

left half of Fig. 5, we show the angular distribution datum for $\gamma_{387.6}$, both from Table I for the $^{92}\text{Zr}(^{13}\text{C}, 3n\gamma)^{102}\text{Pd}$ and from Table II for the $^{94}\text{Zr}(^{12}\text{C}, 4n\gamma)^{102}\text{Pd}$ reaction. These data show that $\gamma_{387.6}$ must be a $J=9-8$ transition, and not $8-8$, with a small ($|\delta| < 0.3$) or zero value of the quadrupole-dipole mixing ratio δ . The right half of Fig. 5 shows that the parity is odd, leading to the assignment $J^\pi=9^-$ to the 3727.9-keV level. Hence the levels at 4432.9, 5325.9, 6344.9, and 7461.7 keV in ^{102}Pd are all odd-spin and odd-parity levels as shown in Fig. 2.

Now we consider the levels of the cascade in ^{102}Pd at the right side of Fig. 2 beginning with the 2138.4-keV level. This level is also populated by the EC- β^+ decay³⁸⁻⁵⁰ of ^{102}Ag to ^{102}Pd and has previously been assigned $J^\pi=4^+$. This is in good agreement with our angular distribution and linear polarization data as listed in Tables I and II which indicate that $\gamma_{1581.9}$ is a stretched $E2$ transition to the $J^\pi=2^+$ first excited state. This spin assignment (but not the parity) was also deduced previously from the $^{99}\text{Ru}(\alpha, n\gamma)^{102}\text{Pd}$ work.¹² Proceeding from this, the level at 2474.4 keV depopulates mainly by $\gamma_{336.4}$, which from Table I appears to be a stretched $E1$ transition, and is populated mainly by $\gamma_{714.0}$ and $\gamma_{440.0}$. The 714.0- and 539.7-keV transitions successively depopulate the level at 3727.9 keV with $J=9^-$ which has already been discussed. From Table I, the 539.7-keV transition appears to be a stretched $E2$ transition. Although $\gamma_{714.0}$ is obscured (by $\gamma_{714.9}$), it is possible that it is also a stretched $E2$ transition. Hence, $J^\pi=5^-$ is indicated for the 2474.4-keV level as is shown in Fig. 2. A difficulty with this assignment arises from the fact that the linear polarization of $\gamma_{1198.3}$ which also depopulates the 2474.4-keV level is negative, whereas a stretched $E1$ transition depopulating an aligned nuclear state has positive linear polarization. The situa-

tion is summarized in Fig. 6. Notice in Fig. 6(c) that the experimental linear polarization -0.28 ± 0.29 for $\gamma_{1198.3}$ is about 2 standard deviations away from the value expected for a stretched pure $E1$ transition. However, if the level at 2474.4 keV instead would be assigned $J^\pi=5^+$, then the linear polarization for $\gamma_{336.4}$ would deviate by 20 standard deviations. Hence, the $J^\pi=5^-$ assignment is favored for the 2474.4-keV level, but one should be aware of the difficulty concerning the linear polarization of $\gamma_{1198.3}$ in ^{102}Pd . Now we consider the level at 2914.4 keV in ^{102}Pd which is depopulated mainly by the 440.0-keV transition. This level has a spin of $J=5, 6$, or 7 since it is promptly fed by $\gamma_{274.0}$ and promptly depopulated by $\gamma_{440.0}$. A spin of $J=7$ can be ruled out, however, since $\gamma_{440.0}$ does not have a negative value of A_4/A_0 , as shown in Tables I and II, corresponding to a stretched quadrupole transition. A spin of 5 is also ruled out since $\gamma_{274.0}$ does not appear to be a stretched quadrupole transition from the data listed in Tables I and II. From the data shown in Fig. 6, $J^\pi=6^-$ is inferred for the 2914.4 keV level and $\delta=+0.40 \pm 0.09$ for $\gamma_{440.0}$. Consequently we conclude that $\gamma_{274.0}$ is a $7^- \rightarrow 6^-$ transition. This is in agreement with the measured quantities shown in Table I for $\gamma_{274.0}$ if $\gamma_{274.0}$ is an $M1-E2$ mixture with a small positive value of δ ($\delta \approx +0.2$; see Ref. 37 for the phase convention).

The cascade 1003.1, 890.7, 776.7, 647.2, and 756.2 keV in ^{102}Pd probably consists of stretched $E2$ transitions. Three difficulties are the DCO ratios of $R=2.13 \pm 0.46$ for $\gamma_{1003.1}$, $R=0.68 \pm 0.14$ for $\gamma_{890.7}$, and $R=1.39 \pm 0.20$ for $\gamma_{756.2}$ (instead of $R=1$ for all three). The R value for $\gamma_{1003.1}$ might have been increased by the removal of coincident intensity (due to Doppler shifting in the Ge(Li) detector at 0°) to a higher energy not contained in the coincident gate. The analysis of $\gamma_{756.2}$ and $\gamma_{890.7}$ is complicated by other overlapping peaks.

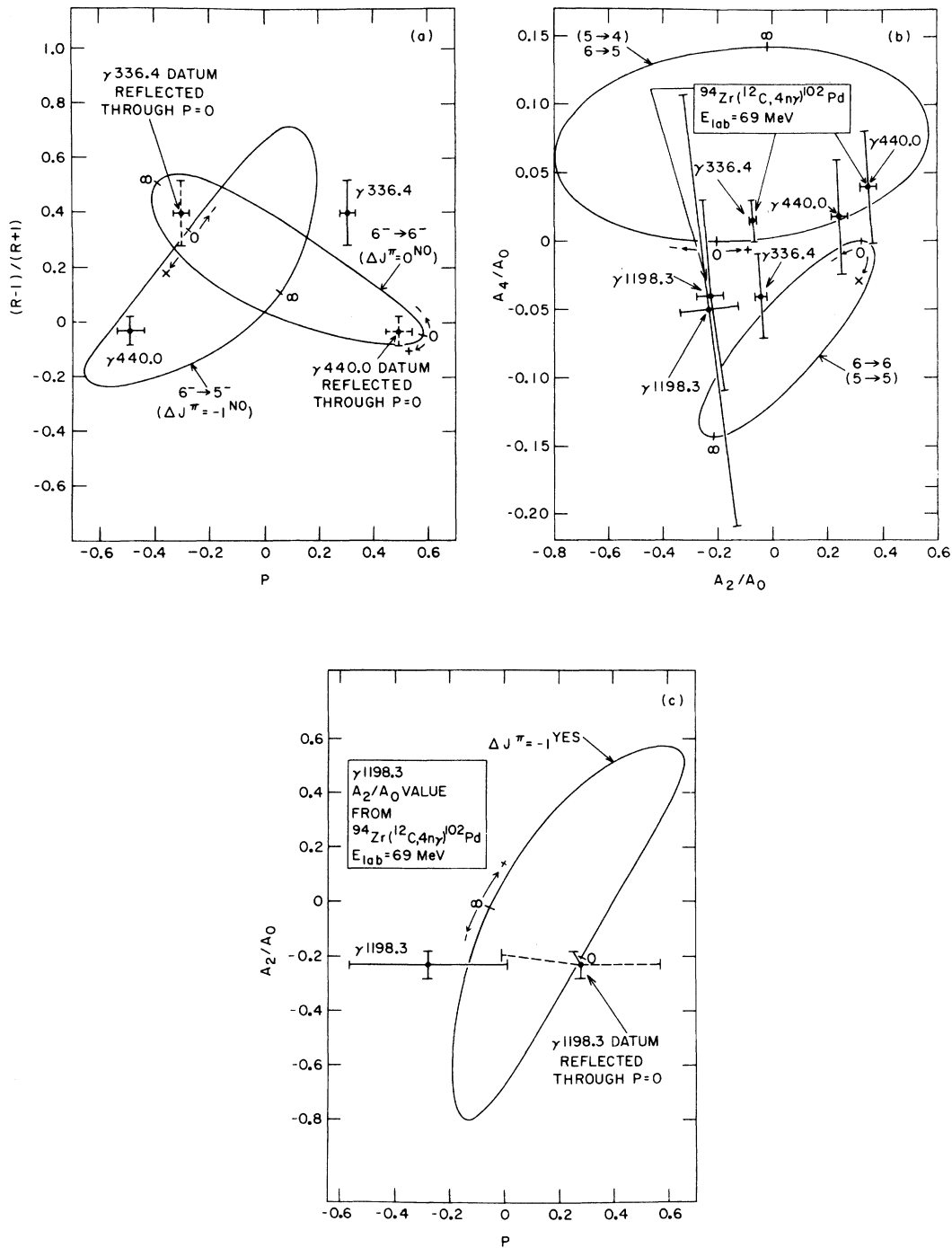


FIG. 6. The possible nuclear spin changes associated with the 336.4-, 440.0-, and 1198.3-keV transitions in ^{102}Pd . These transitions are produced by $^{92}\text{Zr}(^{13}\text{C}, 3n\gamma)$ with $E_{\text{lab}} = 56 \text{ MeV}$. The curves are calculated by assuming a Gaussian magnetic substate population (Ref. 37) of nuclear spins with the following alignment coefficients: the values $\alpha_2 = 0.65$ and $\alpha_4 = 0.23$ are used for the $P, A_2/A_0$, and A_4/A_0 axes, while the values $\alpha_2 = 0.74$, $\alpha_4 = 0.62$, and $\alpha_6 = 0.25$ are used for the $(R-1)/(R+1)$ axis. Along each closed curve, the quadrupole-dipole mixing ratio varies from 0 to $+\infty$ and from 0 to $-\infty$. The spin assignments which follow from these data are discussed in the text. Also shown are data obtained by the $^{94}\text{Zr}(^{12}\text{C}, 4n\gamma)^{102}\text{Pd}$ reaction with $E_{\text{lab}} = 69 \text{ MeV}$.

We note that $\gamma_{1003,1}$, $\gamma_{890,7}$, and $\gamma_{756,2}$ were also previously reported¹⁸ to be stretched quadrupoles. The 482.5-keV transition, therefore, is a mixed $M1$ - $E2$ transition with $\delta \approx +1$. Thus the spin and parity assignments shown in Fig. 2 are considered to be the most probable ones.

The level at 4328.5 keV in ^{102}Pd is depopulated by two transitions $\gamma_{335,8}$ and $\gamma_{988,3}$, that can be placed with confidence and, in addition, two other transitions $\gamma_{1315,8}$ and $\gamma_{600,6}$ whose placement is less certain. For this level, the possible spins are $J = 8, 9$, or 10 . This level has previously been assigned (Ref. 16) $J^\pi = 10^+$; however, that assignment does not seem straightforward to us. A consideration of the present data for $\gamma_{988,3}$ and $\gamma_{335,8}$ reveals that the J^π values for this level arising from an analysis of $\gamma_{988,3}$ could also be $J^\pi = 8^+$ (small negative value for the mixing ratio for $\gamma_{988,3}$) or $J^\pi = 9^+$ (small positive value for the mixing ratio). Further, the values for A_2/A_0 for $\gamma_{988,3}$ from Tables I and II, $+0.02 \pm 0.11$ and 0.06 ± 0.06 , deviate from those expected for a stretched quadrupole transition. The data do not lead to a definite J^π assignment, but because of systematics¹⁶ the assignments of $J^\pi = (10^+)$ for the 4328.5-keV level and $J^\pi = (12^+)$ for the 5260.4-keV level may be upheld.

The level at 3889.5 keV is depopulated by $\gamma_{701,1}$, a stretched $E2$ transition. This level is probably fed by $\gamma_{428,5}$ as shown in Fig. 2. The level at 2651.7 keV was more strongly populated in the previous¹² $^{99}\text{Ru}(\alpha, n\gamma)^{102}\text{Pd}$ work. The possible spins are $J = 4$ or 5 . We rule out $J = 6$ since $\gamma_{1375,8}$ does not have a negative value for A_4/A_0 which would be characteristic of a stretched quadrupole transition. Taking into account the angular distribution data and the linear polarization measurement for $\gamma_{1375,8}$ listed in Tables I and II as well as the previous angular distribution data,¹² the two remaining possibilities are $J^\pi = 4^+$ (in which case $\gamma_{1375,8}$ is pure $M1$) or $J^\pi = 5^-$ (in which case $\gamma_{1375,8}$ is an $E1$ - $M2$ mixture with $\delta \approx +0.1$) for the 2651.7-keV level. The $J^\pi = (4^+)$ assignment is somewhat more probable.

Now we consider the level at 2294.5 keV. This level was not reported in a study⁴⁸ of the $\text{EC}-\beta^+$ decay of ^{102}Ag , but was reported in the $^{99}\text{Ru}(\alpha, n\gamma)^{102}\text{Pd}$ study¹² and assigned 6^+ as well as in the $^{92}\text{Zr}(^{13}\text{C}, 3n\gamma)^{102}\text{Pd}$ study,¹⁶ but assigned 4^- . Figure 2 indicates that the possible spins for this level are $J = 4$ or 5 . A spin of $J = 4$ is unlikely since the transition to the $J^\pi = 2^+$ level at 556.5 keV would have been expected if $J^\pi = 4^+$ while, on the other hand, a $J^\pi = 4^-$ assignment would be contrary both to the observed linear polarization of $\gamma_{1018,6}$ and of $\gamma_{620,0}$ (although both values may be perturbed by overlapping transitions). An assignment of J^π

$= 5^+$ would be mildly contrary to the observed A_2/A_0 value for $\gamma_{620,0}$ which would then be mostly $E1$, the A_2/A_0 value of $\gamma_{182,4}$, and the linear polarization of $\gamma_{1018,6}$. An assignment of $J^\pi = 5^-$, however, while being in agreement with an $M1$ - $E2$ mixing ratio $\delta \approx +0.1$ for $\gamma_{620,0}$ would not be in agreement with the observed linear polarization of $\gamma_{620,0}$ as can be seen from the curves shown in Fig. 6(a). This last assignment would also not agree with the linear polarization for $\gamma_{179,8}$ nor with the observed value of A_2/A_0 for $\gamma_{182,4}$. In view of this difficulty, we cannot make a definite spin and parity assignment for the 2294.5-keV level but merely suggest $J^\pi = (5^+)$. Another possibility, which is not ruled out by our coincidence data, is that there are two nearly degenerate levels at 2294.5 keV in ^{102}Pd . The first level (at 2294.5 keV) would be fed by $\gamma_{179,8}$ and $\gamma_{620,0}$ and in turn would be depopulated by $\gamma_{1018,6}$ ($\gamma_{1018,6}$ and $\gamma_{179,8}$ are observed in coincidence). The other level (at 2295.0 keV) would be depopulated by $\gamma_{182,4}$. We emphasize that we do not have any direct evidence for two nearly degenerate levels at 2294.5 keV, but are puzzled by the data concerning this level.

Now we consider the level at 2112.4 keV shown in Fig. 2. The three transitions $\gamma_{182,4}$, $\gamma_{1556,1}$, and $\gamma_{556,5}$ are observed in coincidence with each other. However, there is another "183 keV" transition which we are not able to place in the ^{102}Pd level scheme. This other 183 keV transition has previously been assigned¹² as a $J = 6$ (2294.5 keV) to $J^\pi = 6^+$ (2111.3 keV) transition on the basis of an observed weak coincidence between " γ_{183} " and " γ_{835} ." However, we did not observe $\gamma_{440,4} - \gamma_{835,5}$ coincidence events nor $\gamma_{183} - \gamma_{835,4}$ events to an extent allowing us to definitely place this other γ_{183} in the same location as was previously proposed.¹² The previously observed $\gamma_{183} - \gamma_{835}$ weak coincidence events may have resulted from $\gamma_{182,4}$ shown in Fig. 2 and an 836 keV transition from the 2112.4 keV level to the $J^\pi = 4^+$ level at 1275.9 keV excitation. However, we have no direct evidence for or against such an 836 keV transition which would overlap in energy with the more intense $6^+ \rightarrow 4^+$ transition of the ground state cascade. Recently, a study⁵¹ of the excitation of ^{102}Pd with 8 MeV protons has shown that this state can only have $J^\pi = 3^{(+)}$. This assignment is in agreement with the data shown in Tables I and II and with a previous assignment.¹⁶

For completeness, we have included several levels for ^{102}Pd in Fig. 2 which are not strongly populated in the present work but whose existence has been inferred from previous studies. The 1918 keV level was deduced¹² from the $^{99}\text{Ru}(\alpha, n)^{102}\text{Pd}$ data, but no J^π value was assigned. There

are four additional levels shown in Fig. 2 inferred from studying⁴⁸ the EC- β^+ decay of ^{102}Ag : 1535.2, 2799.0, 2716.5, and 3238.6 keV. These have previously been assigned J^π values of 2^+ , 4^+ , $(1^+, 2^+)$, and $(1^+, 2^+)$, respectively. Moreover, a $J^\pi = 0^+$ 1592.5 keV level is shown in Fig. 2, which was inferred from an in-beam internal conversion study^{49,50} of the decay of ^{102}Ag to ^{102}Pd . This $J^\pi = 0^+$ level might be a member of the two-phonon triplet of states in ^{102}Pd . Finally, several new levels in ^{102}Pd have been found recently from the study⁵¹ of the inelastic scattering of 8 MeV protons from ^{102}Pd . In particular, a $J^\pi = 0^+$ level at 1658 keV, a $J^\pi = 2^+$ level at 1944 keV, and 18 additional new levels between 2.2 MeV and 3.2 MeV excitation energy have been found. These 20 levels have not been included in Fig. 2.

B. ^{100}Pd

Now we consider the level scheme for ^{100}Pd shown in Fig. 4. No excited states in ^{100}Pd were known prior to the present work.⁴ However, two transitions of 665.8 and 750.4 keV were found⁵² following the decay of ^{100}Ag with a half-life of 1.9 ± 0.3 min. We find that these two transitions are produced promptly by $^{12}\text{C} + ^{91}\text{Zr}$ (enriched to

88%) with $E_{\text{lab}} = 63$ MeV. Moreover, these two transitions are observed to be the two strongest members of the following coincident cascade of γ -rays: 945.4, 892.0, 881.3, 798.6, 773.0, 750.5, and 665.3 keV. This cascade of seven transitions, arranged according to intensity, is shown in Fig. 4. The transition energies and the relative intensities from $^{12}\text{C} + ^{91}\text{Zr}$ at $E_{\text{lab}} = 63$ MeV are listed in the first two columns of Table III. The angular distribution coefficients are listed in the third and fourth columns of Table III while the experimental correlation ratios R and the linear polarization results are listed in the fifth and seventh columns, respectively. An additional angular distribution experiment was performed using $^{12}\text{C} + ^{91}\text{Zr}$ with $E_{\text{lab}} = 56$ MeV. The results are listed in Table IV. The seven transitions of the ground-state cascade are all stretched $E2$ transitions. Therefore, this cascade ($\Delta J = 2$) connects a set of positive-parity even-spin levels up to $J^\pi = 14^+$.

The level at 3177.1 keV shown in Fig. 4 is fed by $\gamma_{969.1}$ and $\gamma_{805.4}$, and is depopulated by $\gamma_{189.6}$ and $\gamma_{988.6}$. The possible spins are $J = 7$ or 8 . A spin of $J = 6$ is ruled out since, in that event, $\gamma_{189.6}$ would be a stretched quadrupole transition.

TABLE III. Transitions in ^{100}Pd produced by 63 MeV $^{12}\text{C} + ^{91}\text{Zr}$. The correlation ratio R is defined by Eq. (2) and M is the number of coincident stretched $E2$ transitions used to determine R .

Transition energy (keV)	Relative intensity	A_2/A_0	A_4/A_0	R	M	Linear polarization P	Assignment
189.64 ± 0.29	7.3 ± 0.9^a	0.216 ± 0.008	-0.010 ± 0.012	$1.61^{+0.50}_{-0.35}$	4		$8^- \rightarrow 8^+$
277.33 ± 0.52	5.6 ± 0.9^a			0.75 ± 0.24	4		$(10^+) \rightarrow 10^+$
467.37 ± 0.49	4.0 ± 1.0^a			$2.9^{+2.0}_{-0.9}$	6		$(\rightarrow 5452.1 \text{ keV level})$
479.59 ± 0.29	2.82 ± 0.31	-0.32 ± 0.09	0.10 ± 0.12	1.4 ± 0.8	7	-0.75 ± 0.25	$(\rightarrow 14^+)$
665.32 ± 0.12	$\equiv 100.0 \pm 2.1$	0.269 ± 0.005	-0.089 ± 0.007			0.526 ± 0.035	$2^+ \rightarrow 0^+$
691.45 ± 0.38	4.7 ± 1.2	-0.108 ± 0.020	-0.003 ± 0.029	$1.8^{+0.8}_{-0.4}$	6		$(\rightarrow 12^+)$
725.84 ± 0.35	12.0 ± 1.7^a	0.172 ± 0.017	-0.080 ± 0.024	1.24 ± 0.35	2	0.26 ± 0.10^b	$7^- \rightarrow 5^-$
750.48 ± 0.12	87.2 ± 1.5	0.269 ± 0.012	-0.083 ± 0.018	1.13 ± 0.08	1	0.369 ± 0.037	$4^+ \rightarrow 2^+$
773.05 ± 0.12	82.9 ± 1.9	0.298 ± 0.007	-0.078 ± 0.009	0.97 ± 0.06	2	0.480 ± 0.038	$6^+ \rightarrow 4^+$
798.58 ± 0.14	53.2 ± 1.7	0.322 ± 0.009	-0.119 ± 0.012	0.90 ± 0.06	3	0.454 ± 0.061	$8^+ \rightarrow 6^+$
805.43 ± 0.18	15.8 ± 1.0^a	0.312 ± 0.007	-0.121 ± 0.010	0.93 ± 0.12	5	0.42 ± 0.07^b	$10^- \rightarrow 8^-$
809.39 ± 0.14	14.0 ± 1.1	0.309 ± 0.025	-0.160 ± 0.035	1.01 ± 0.10	6	0.37 ± 0.12	$12^- \rightarrow 10^-$
862.08 ± 0.34	7.1 ± 1.1^a			$1.7^{+0.7}_{-0.4}$	3		$(9^-) \rightarrow 7^-$
875.48 ± 0.58	7.0 ± 0.8^a			2.23 ± 0.68	3		$(19^-) \rightarrow 18^-$
881.33 ± 0.18	34.9 ± 1.3^a	0.309 ± 0.018	-0.120 ± 0.025	1.18 ± 0.09	4	0.54 ± 0.05	$10^+ \rightarrow 8^+$
891.95 ± 0.16	24.3 ± 1.1^a	0.332 ± 0.019	-0.088 ± 0.027	1.08 ± 0.10	5	0.48 ± 0.09^b	$12^+ \rightarrow 10^+$
940.17 ± 0.27	10.5 ± 0.9^a	0.279 ± 0.019	-0.120 ± 0.027	0.93 ± 0.11	7	0.34 ± 0.11^b	$14^- \rightarrow 12^-$
945.43 ± 0.42	11.1 ± 0.9^a	0.262 ± 0.015	-0.115 ± 0.012	0.96 ± 0.15	6	0.53 ± 0.13^b	$14^+ \rightarrow 12^+$
969.09 ± 0.58	4.08 ± 0.31	0.51 ± 0.16	-0.16 ± 0.28	1.2 ± 0.6	4		$(10^+) \rightarrow 8^-$
988.55 ± 0.56	5.24 ± 0.34	0.349 ± 0.025	-0.095 ± 0.035	1.01 ± 0.33	3	-0.33 ± 0.37	$8^- \rightarrow 6^+$
1035.87 ± 0.21	11.7 ± 0.9^a	0.253 ± 0.055	-0.158 ± 0.078	1.10 ± 0.13	8	0.70 ± 0.18	$16^- \rightarrow 14^-$
1070.96 ± 0.48	6.4 ± 1.0^a	0.15 ± 0.09	-0.19 ± 0.13	1.33 ± 0.31	9	0.49 ± 0.20	$18^- \rightarrow 16^-$
1089.09 ± 0.28	14.36 ± 0.48	-0.231 ± 0.025	-0.006 ± 0.035	$3.6^{+1.5}_{-0.8}$	2	0.42 ± 0.20	$5^- \rightarrow 4^+$

^a This transition is unresolved from other transitions. The intensity is deduced from coincident data.

^b This value may be perturbed by unresolved transitions.

TABLE IV. Transitions in ^{100}Pd produced by 56 MeV $^{12}\text{C} + ^{91}\text{Zr}$. The intensities have been corrected for the Ge(Li) detector efficiency and the A_2/A_0 and A_4/A_0 values have been slightly corrected for the finite solid angle of the detector.

Transition energy (keV)	Relative intensity	A_2/A_0	A_4/A_0
189.64	<17	0.306 ± 0.022 §	-0.005 ± 0.032 §
277.33	6.38 ± 0.35	0.41 ± 0.06	-0.10 ± 0.09
467.37	<17	0.20 ± 0.09 §	-0.13 ± 0.13 §
479.59	3.68 ± 0.32	0.03 ± 0.09	-0.09 ± 0.13
665.32	100.0 ± 1.7	0.277 ± 0.013	-0.062 ± 0.018
691.45	5.67 ± 0.62	-0.08 ± 0.08	0.08 ± 0.12
725.84	<20	0.234 ± 0.028 §	-0.025 ± 0.041 §
750.48	<99	0.290 ± 0.010	-0.068 ± 0.015
773.05	71.5 ± 1.0	0.317 ± 0.013	-0.078 ± 0.018
798.58	50.7 ± 1.1	0.307 ± 0.012	-0.062 ± 0.017
805.43	6.6^b	0.307 ± 0.026 §	-0.039 ± 0.038 §
809.39	12.36 ± 0.41	0.336 ± 0.041	-0.064 ± 0.060
862.08	11^c	0.191 ± 0.029 §	-0.104 ± 0.043 §
875.48	<28	0.090 ± 0.023 §	0.000 ± 0.035 §
881.33	41.8 ± 1.8^a	0.288 ± 0.018 §	-0.116 ± 0.026 §
891.95	20.7^d	0.358 ± 0.017 §	-0.102 ± 0.025 §
940.17	3.8 ± 0.8	0.289 ± 0.047	-0.150 ± 0.069
945.43	9.5 ± 1.5	0.34 ± 0.06	-0.11 ± 0.09
969.09	4.70 ± 0.23^e	0.46 ± 0.08	-0.15 ± 0.12
988.55	5.25 ± 0.21^f	0.33 ± 0.06	-0.03 ± 0.09
1035.87	8.03 ± 0.35	0.29 ± 0.07	-0.02 ± 0.10
1070.96	<4		
1089.09	14.55 ± 0.36	-0.274 ± 0.039	0.019 ± 0.058

^a Corrected for 10% contribution from a ^{99}Pd transition.

^b Corrected for 31% contribution from a ^{101}Pd transition.

^c Corrected for 50% contribution from a ^{99}Rh transition.

^d Corrected for 15% contribution from ^{99}Rh and 10% from ^{101}Pd transitions.

^e Corrected for 7% contribution from a ^{108}Pd transition.

^f Corrected for 4% contribution from a ^{108}Pd transition.

§ This value may be perturbed by unresolved transitions.

This would be in disagreement both with the A_4/A_0 value of -0.010 ± 0.012 shown in Table III for $\gamma_{189.6}$ (A_4/A_0 would be ≈ -0.12 for a stretched quadrupole) and with the correlation ratio value of $R = 1.61^{+0.50}_{-0.35}$ ($R = 1$ for a stretched quadrupole). We have performed lifetime measurements utilizing a pulsed ^{12}C beam and find that $\gamma_{189.6}$ is produced promptly. This observation rules out an appreciable octupole admixture for $\gamma_{189.6}$. Therefore, $J = 9$ is also ruled out for the 3177.1 keV level. A $J = 7$ assignment is also not allowed since, in that event, $\gamma_{988.6}$ would be expected to have a non-negative value for A_4/A_0 for all values of the quadrupole-dipole mixing ratio, while the experimental value is $A_4/A_0 = -0.095 \pm 0.035$ as listed in Table III. The only remaining possibility $J = 8$ is in agreement with the angular distribution data and with the correlation ratio listed in Table III for $\gamma_{988.6}$ (stretched quadrupole) and for $\gamma_{189.6}$ ($|\delta| < 0.1$). The linear polarization measurement listed in Table III for $\gamma_{988.6}$ of $P = -0.33 \pm 0.37$ indicates that this transition is $M2$. Therefore, $J^\pi = 8^-$ is the

most probable assignment for the 3177.1-keV level in ^{100}Pd . The linear polarization of $\gamma_{189.6}$ could not be determined because of the presence of (at least) three overlapping peaks from transitions in other nuclides.

The levels at 7839.0, 6768.0, 5732.1, 4791.9, 3982.5, and 3177.1 keV shown in Fig. 4 are connected by stretched $E2$ transitions. These assignments are in agreement with the data listed in Tables III and IV for the transitions $\gamma_{805.4}$, $\gamma_{809.4}$, $\gamma_{940.2}$, $\gamma_{1035.9}$, and $\gamma_{1071.0}$. We have placed $\gamma_{1035.9}$ above $\gamma_{940.2}$ in the ^{100}Pd level scheme even though the former transition appears to be slightly more intense as can be seen from Table III. This switch is suggested by the sequence of increasing transition energies and is not ruled out by the errors in the intensities listed in Table III. On the other hand, Table IV suggests that $\gamma_{1035.9}$ is about twice as intense as $\gamma_{940.2}$. However, it is difficult to extract a precise intensity for $\gamma_{940.2}$ from singles data due to the existence of other transitions overlapping in energy as may be seen

in Fig. 3. We mention one possibility that comes to mind, namely that the 5732.1 keV level in ^{100}Pd is depopulated by at least one hitherto undiscovered transition in addition to $\gamma_{940.2}$. The analog of this occurs for the 4318.0 keV level in ^{102}Pd as has been discussed above. In this event, $\gamma_{1035.9}$ might be observed more intensely than $\gamma_{940.2}$ even though the ordering in fact is as shown in Fig. 4. These levels, therefore, form an even-spin odd-parity sequence: $J^\pi = 8^-, 10^-, 12^-, 14^-, 16^-$, and 18^- . An 875.5 keV γ ray is observed in coincidence with all five of the transitions in ^{100}Pd which belong to this even-spin odd-parity cascade. This suggests the existence of an 8714.5 keV level in ^{100}Pd . The angular distribution coefficients for this transition are severely perturbed by other overlapping transitions. The correlation ratio measurement $R = 2.23 \pm 0.68$ suggests that $\gamma_{875.5}$ is not a stretched quadrupole transition. Therefore the spin of the 8714.5 keV level could only be $J = 17, 18$, or 19 . A spin of 17 is improbable since a transition to the $J^\pi = 16^-$ level at 6768.0 keV is not observed. We suggest a spin of 19 for the 8714.5-keV level as the most probable choice.

The level at 2504.9 keV is depopulated by the 1089.1 keV transition to the $J^\pi = 4^+$ member of the ground state cascade. The 2504.9-keV level can only have $J^\pi = 5^-$ or 3^- , as follows from the data for $\gamma_{1089.1}$ in Tables III and IV. However, no transition from the 2504.9-keV level to the $J^\pi = 2^+$ level is observed. This suggests $J^\pi = 5^-$ and not 3^- for the 2504.9-keV level. The levels at 4092.8 and 3230.7 keV are depopulated by $\gamma_{862.1}$ and $\gamma_{725.8}$, respectively. Both of the transitions are probably stretched $E2$ transitions, although the data for both transitions are perturbed by other unresolved transitions. The most likely spin-parity assignment for the 3230.7-keV level is $J^\pi = 7^-$. With less confidence, we propose $J^\pi = (9^-)$ for the 4092.8-keV level.

The level at 4146.1 keV shown in Fig. 4 is depopulated both by $\gamma_{277.3}$ to the $J^\pi = 10^+$ member of the ground state band and by $\gamma_{277.3}$ to the level with $J^\pi = 8^-$ at 3177.1 keV. Hence, this level can only have a spin of $J = 8, 9$, or 10 . However, the data for both transitions are obscured by other overlapping γ -ray peaks. Therefore, we can only suggest $J^\pi = (10^+)$ for the 4146.1 keV level in ^{100}Pd , with $J^\pi = 8^+$ or 8^- also being possible.

There are three remaining transitions shown in the ^{100}Pd level scheme which we have not yet discussed: $\gamma_{691.4}$, $\gamma_{466.0}$, and $\gamma_{479.6}$. These are weak transitions which can definitely be assigned to ^{100}Pd on the basis of γ - γ coincidence data. However, the determination of the level of the ground state band at which these transitions feed is only tentative. We have dashed the levels in Fig. 4

whose existence is tentative. This completes the discussion of the analysis of the data for the observed transitions in ^{102}Pd and ^{100}Pd .

DISCUSSION

We now describe several methods of calculating the observed energy levels and branching ratios. Iachello, Feshbach, and Arima have proposed that nuclei which are not too near closed shells and do not have too large a deformation might be described^{30,31} as a boson gas. Such a description would lend insight concerning the collective states in ^{100}Pd and ^{102}Pd . However, one expects that at least some states of these nuclei are more easily described as shell model states, for example, two quasineutron states. The first problem is that we do not know which of the states are collective—that is, they cannot be accurately described as the motion of only four or fewer quasiparticles—and which are not.

To start, we suppose that the excited states of ^{100}Pd and ^{102}Pd are collective levels composed of several quadrupole and octupole bosons. The bosons are allowed to interact (in a way that does not change the number of bosons), otherwise, the vibrational limit would emerge with the $J^\pi = 4^+$ state at twice the excitation energy of the 2^+ state. Iachello and Arima³⁰ have worked out the energy values for those positive parity states composed by coupling only quadrupole bosons

$$E(n, \nu, n_\Delta, L, M) = \epsilon_2 N + \frac{\alpha}{2} N(N-1) + \beta(N-\nu)(N+\nu+3) \\ + \gamma[L(L+1) - 6N], \quad N=0, 1, 2, \dots, \quad (4)$$

where ϵ_2 is the energy of a quadrupole boson, N is the boson number, ν is the seniority, n_Δ counts boson triplets coupled to zero angular momentum, L is the angular momentum, and M is its component along an axis. They label the ground state band the "Y" band for which $\nu = N$, $n_\Delta = 0$, and $L = 2N$ for $N = 0, 1, 2, \dots$, and the energies are

$$E_Y(L=2N) = \frac{1}{8}(4\epsilon_2 - 3C_4^{22})L + \frac{C_4^{22}}{8}L(L+1), \\ L=0, 2, 4, \dots, \quad (5)$$

where we shall consider ϵ_2 and C_4^{22} to be adjustable parameters. Notice that the angular momentum dependence of Eq. (5) is the same as that proposed several years ago by Ejiri.⁵³ Equation (5) can be rewritten as

$$E_Y(L=2N) = \epsilon_2 N + C_4^{22} \frac{N(N-1)}{2}, \quad N=0, 1, 2, \dots, \quad (6)$$

from which it is clear that C_4^{23} is responsible for the deviations of the energies of the calculated ground state band from those of a harmonic vibrator. There are many other boson states besides the "Y" band which can be formed from quadrupole bosons, but we shall not need them here. Negative parity states can be formed,³² for example, by coupling one octupole boson to one or more quadrupole bosons. We shall utilize the "totally aligned" band whose energies are

$$E(J=2N+3) = E_Y(L=2N) + \epsilon_3 + NC_5^{23}, \quad N=0, 1, 2, \dots, \quad (7)$$

where $E_Y(L=2N)$ is given by Eq. (5). We shall consider ϵ_3 and C_5^{23} to be adjustable parameters. The remaining band³² we shall utilize is the "totally aligned minus one" band with energies given by

$$E(J=2N+2) = E_Y(L=2N) + \epsilon_3 + NC_5^{23} + \frac{1}{5}(2N+3)\Delta_4^{23}, \quad N=1, 2, \dots, \quad (8)$$

where Δ_4^{23} is an additional adjustable parameter.

In Fig. 2 and Fig. 4, we display the fits to the $J^\pi = 2^+$ and 4^+ members of the ground-state cascades of ^{102}Pd and ^{100}Pd which result from Eq. (5). In both cases, the IBA levels are at a higher energy than experiment. We could greatly reduce the deviation, of course, by fitting Eq. (5) to all of the ground-state-cascade levels up to $J=14^+$, but we have chosen not to in order to display the predictions of IBA for the higher-spin states. A second method we have tried is to fit simultaneously, for each nuclide, Eq. (5) to the ground state cascade and Eqs. (7) and (8) to the observed yrast negative parity states. The results are compared with experiment in Fig. 7 for both ^{100}Pd and ^{102}Pd . Now the IBA levels for the ground state cascades yield better fits than the ones displayed in Fig. 2 and Fig. 4. The IBA levels in Fig. 7 are five-parameter fits to 16 experimental levels in ^{100}Pd or to 20 levels in ^{102}Pd . The overall correspondence is encouraging.

The IBA can also be used³² to calculate branching ratios which can be tested for ^{102}Pd and its isotone (Ref. 54) ^{100}Ru as well as for $^{104,106}\text{Pd}$. These are summarized in Table V. To calculate the experimental $B(E2)$ value for $\gamma_{482.5}$ ($J^\pi = 8^- \rightarrow 7^-$, ^{102}Pd), we use the experimental value $\delta = +1.5 \pm 0.5$ for the $M1-E2$ mixing ratio and for $\gamma_{590.2}$ ($J^\pi = 10^- \rightarrow 9^-$, ^{102}Pd), we use $\delta = +0.14 \pm 0.09$. For ^{100}Ru , we deduce from previous data⁵⁴ a mixing ratio of $\delta = +1.5 \pm 0.8$ for $\gamma_{403.4}$ ($J^\pi = 8^- \rightarrow 7^-$), and we find two possibilities for $\gamma_{489.4}$ ($J^\pi = 10^- \rightarrow 9^-$): either $\delta = +0.34 \pm 0.16$ or $\delta = +6.2 \pm 3.5$. To obtain the IBA predictions,³² we interpret the $J^\pi = 8^-$ and 10^- levels as being members of the "totally aligned

minus one" band while the yrast $J^\pi = 7^-$ and 9^- levels would be members of the "totally aligned" band. The magnitudes of the IBA ratios shown in the third column of Table V are generally smaller than experiment although the trend is correct. The $J^\pi = 7^- \rightarrow 6^+$ transition in ^{102}Pd (1077.1 keV) is conspicuously absent both in Fig. 2 and Table V, unless this is the weak 1076.0 keV transition listed in Table I but not placed in the ^{102}Pd level scheme. The intensity of this 1076.0 keV transition is such that the number $(0.20 \pm 0.03) \times 10^{-5} \text{b}^{-1}$ would have been entered in the ninth column of Table V for $N=2$ (instead of <0.4). The corresponding $J^\pi = 7^- \rightarrow 6^+$ transition is also not seen in ^{100}Pd , whereas it is found to be robust¹⁶ in ^{104}Pd and ^{106}Pd .

It is interesting to compare the IBA description of these levels to the description given by the two-parameter variable moment of inertia (VMI) model.^{1,2} The VMI energies for states of spin J belonging to the same band are given by

$$E_J = \frac{1}{2}C(\mathcal{J}_J - \mathcal{J}_0) + \frac{J(J+1)}{2\mathcal{J}_J}, \quad J=0, 2, 4, \dots, \quad (9)$$

with the equilibrium constant $\partial E_J / \partial \mathcal{J}_J = 0$ fixing the moment of inertia \mathcal{J} for each level. In Figs. 2 and 4, we display the VMI predictions for the ground state bands of ^{102}Pd and ^{100}Pd , respectively. These levels are fits just to the yrast $J^\pi = 2^+$ and 4^+ levels as was done for the IBA fits. The VMI model does much better than the IBA model for ^{102}Pd but only about the same as the IBA model for ^{100}Pd . Of course, both the VMI model and the IBA model can be fit to all seven ground state band levels giving much improved fits for each nuclide. The resulting fits are comparable to each other and to (the appropriate part of) the IBA fits already shown in Fig. 7.

We mention here the results of a recent calculation by Hsu *et al.*⁵⁵ of the energies of states of the even-Pd nuclides from $A=102$ to $A=114$. That calculation utilizes a collective model which includes rotations and vibrations of a deformed nucleus. Although the larger number (≈ 5) of parameters used by Hsu *et al.* makes it difficult to compare their results in detail with either VMI or IBA, we mention that they find⁵⁵ that ^{102}Pd and ^{100}Pd are "softer" towards permanent deformation than any of the heavier even-Pd nuclides, in agreement with the VMI model.^{1,2}

A third description of these levels comes from the deformed shell model. For this, we attempt to describe the yrast states of ^{100}Pd and ^{102}Pd as two valence quasineutrons in Nilsson orbitals plus an inert slightly deformed core.⁵⁶⁻⁵⁸ We further suppose that the effect of adding angular momentum to the axially symmetric nucleus may be described by the Coriolis force—as has been done

many times in the literature. We shall, moreover, include an elastic-energy term

$$\frac{1}{2}C(\vartheta - \vartheta_0)^2 \quad (10)$$

as was done for the VMI model^{1,2} and as was also recently done⁵⁹ by Smith and Rickey for a calculation of level energies in the odd- A nuclides^{101,103,105}Pd. We shall consider C as a parameter to be adjusted for each nuclide in order to reproduce the experimental level energies. Therefore, we take as a Hamiltonian,⁵⁷

$$H = H_P + H_C + \frac{\hbar^2}{2\mathcal{I}} [J(J+1) + \vec{j}^2 - 2K^2] + \frac{1}{2}C(\vartheta - \vartheta_0)^2, \quad (11)$$

where H_P is the Hamiltonian of the valence neutrons in the absence of rotation, H_C is the "Coriolis" operator given by

$$H_C = \frac{-\hbar}{2\mathcal{I}} A(j_+ j_- + j_- j_+) f(U, V), \quad (12)$$

where J is the nuclear spin, j is the total valence

neutron spin, K is the projection of J on the nuclear symmetry axis, \mathcal{I} is the nuclear moment of inertia, A is an attenuation factor, and $f(U, V)$ is a pairing factor. Each valence neutron Hamiltonian is

$$H_p = [(\epsilon_p - \lambda)^2 + \Delta^2]^{1/2}, \quad (13)$$

where ϵ_p is the energy of the Nilsson orbital with respect to the neutron Fermi surface λ and 2Δ is the neutron pairing gap. The neutron pairing factor is taken as

$$f(U, V) = \begin{cases} U_1 U_2 + V_1 V_2 & 2 \text{ qp} - 2 \text{ qp}, \\ U_1 V_2 - V_1 U_2 & 0 \text{ qp} - 2 \text{ qp}, \end{cases} \quad (14)$$

where the upper expression is used for the force between one 2-quasiparticle state and another 2-quasiparticle state while the lower expression is used for the force between the 0-quasiparticle state and any 2-quasiparticle state. We allow the nucleus to have β_2 and β_4 deformations.⁵⁸

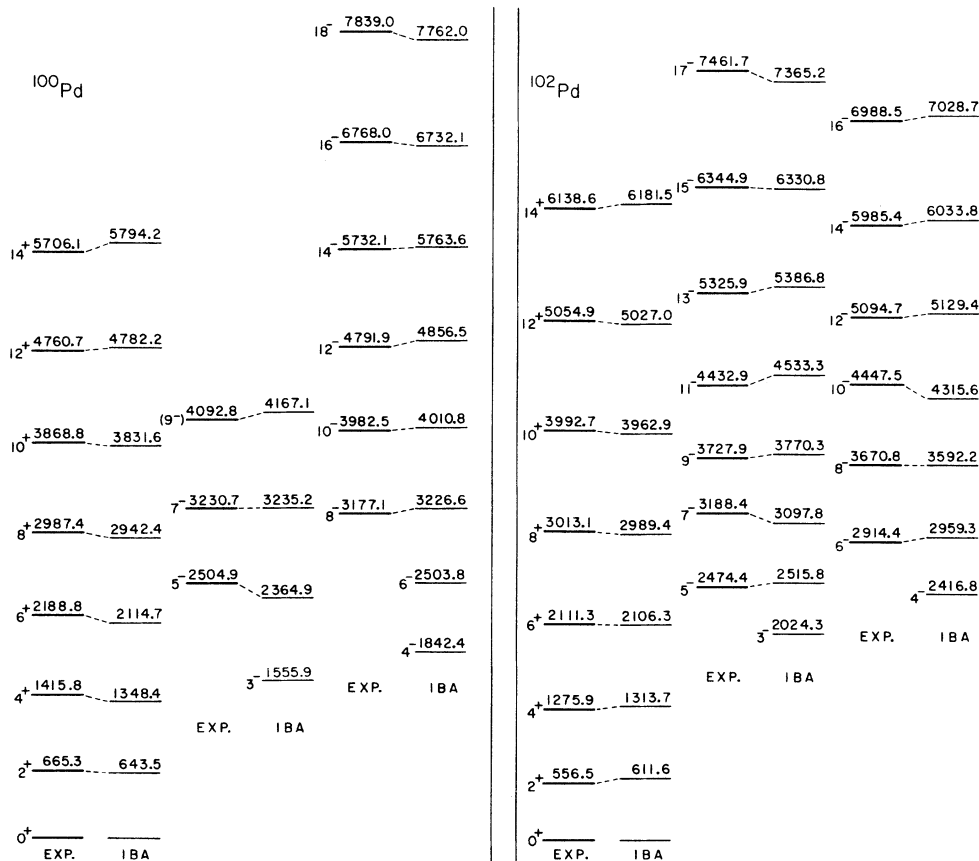


FIG. 7. A comparison of experimental excitation energies of levels in ^{100}Pd and ^{102}Pd with five-parameter fits of the IBA model. For ^{100}Pd , the values of the fitted parameters are (in keV) $\epsilon_2 = 643$, $C_4^{22} = 61.4$, $\epsilon_3 = 1560$, $C_5^{23} = +166$, and $\Delta_4^{23} = -522$. For ^{102}Pd , the fitted parameters are (in keV) $\epsilon_2 = 612$, $C_4^{22} = 90.5$, $\epsilon_3 = 2020$, $C_5^{23} = -120$, and $\Delta_4^{23} = -99.0$. The rms deviation for the 20 calculated levels in ^{102}Pd is 61 keV while for the 16 levels in ^{100}Pd it is 63 keV.

TABLE V. A comparison of four branching ratios in ^{102}Pd to the IBA predictions. The experimental ratios are listed in the fourth and the tenth columns. The IBA predictions (Ref. 32) are given in the third column for the "totally aligned minus one" band and in the ninth column for the "totally aligned" band, respectively. The boson number N and the initial spins J_1 or J_2 are also listed. For comparison, the experimental ratios (Ref. 54) for the isotope ^{100}Ru are listed as well as for (Ref. 19) ^{104}Pd and ^{106}Pd .

N	J_1^-	$\frac{3}{N(N+5)}$	$\frac{B[E_1, J_1^- \rightarrow (J_1-1)^-]}{B[E_2, J_1^- \rightarrow (J_1-2)^-]}$	J_2^-	$\frac{N+1}{N}c$	$\frac{B[E_1, J_2^- \rightarrow (J_2-1)^+]}{B[E_2, J_2^- \rightarrow (J_2-2)^-]}$ ($\times 10^{-5}/b$)	^{102}Pd	^{106}Pd	^{104}Pd	^{100}Pd
2	8^-	0.167	1.7 ± 0.5	7^-	2.09	0.88 ± 0.09	< 0.4	0.24 ± 0.07	5.5 ± 0.3	0.165 ± 0.011
3	10^-	0.091	≈ 0.02	9^-	≈ 1.86	0.17 ± 0.13	1.86 ± 0.23	0.64 ± 0.25	3.26 ± 0.25	
4	12^-	0.058	< 0.7	11^-	1.07	1.39 ± 0.23				

To determine the moments of inertia, which serve as input values to the diagonalization of Eq. (11), we adopt the recipe used by Smith and Rickey.⁵⁹ We notice that the E_{4^+}/E_{2^+} values for both ^{100}Pd and ^{102}Pd are near the value 2.23 for which the ground state moment of inertia \mathcal{I}_0 vanishes according to the VMI model.^{1,2} The VMI equilibrium constraint in this limit becomes

$$2C\mathcal{I}_J^3 = J(J+1), \quad J=2, 4, 6, \dots \quad (15)$$

for the ground state band of an even nuclide. Therefore, we shall use

$$2C\mathcal{I}_J^3 = J(J+1) + \langle \vec{j}^2 \rangle - 2K^2 \quad (16)$$

to calculate the moment of inertia \mathcal{I}_J to use in Eq. (11).

Our procedure is to calculate first the positive and negative parity states for the neighboring odd-mass nuclides $^{99,101,103}\text{Pd}$. The odd- A nuclides are used to determine suitable values for the various parameters such as for the Nilsson model. These parameters are then used without further change to calculate the even- A level energies. Since we are primarily interested here in the even- A nuclides, this method treats these nuclides with a minimum of parameter adjusting while at the same time bringing into play the largest body of empirical information. The results are presented in Figs. 8 and 9. The following describes these calculations in more detail.

First, a Nilsson diagonalization is performed⁶⁰ using the parameters $\mu = 0.40$, $\kappa = 0.074$, $\epsilon_2 = 0.15$, and $\epsilon_4 = 0.0$ for the eleven neutron orbitals whose spherical labels are $h_{11/2}(\Omega = \frac{1}{2}, \frac{3}{2}, \frac{5}{2}, \frac{7}{2})$, $g_{7/2}(\Omega = \frac{1}{2}, \frac{3}{2}, \frac{5}{2}, \frac{7}{2})$, or $d_{5/2}(\Omega = \frac{1}{2}, \frac{3}{2}, \frac{5}{2})$. The results are insensitive to the value of μ used. The effect of increasing κ in this mass region is to lower the negative parity quasineutron energies, given by Eq. (13), relative to the positive parity ones. We have chosen $\kappa = 0.074$ which yields nearly the experimental excitation energy of 784.6 keV for the $J^\pi = \frac{11}{2}^-$ state in ^{103}Pd . We have adopted a value of $\epsilon_2 = 0.15$ for the deformation⁶¹ and have taken $\epsilon_4 = 0.0$ merely because there appears to be insufficient data to estimate this hexadecapole constant. The effect of changing ϵ_2 on the relative energies of the neutron orbitals is described by the familiar Nilsson diagram while the effect of increasing (decreasing) ϵ_4 is to cause an increase (decrease) in the density of orbitals near the Fermi level for the neutrons.

One may wonder, at this point, whether the moderate deformation $\epsilon_2 = 0.15$ which we use is too large. One difficulty, however, which has occurred in a recent calculation of the energy levels of $^{101,103,105}\text{Pd}$ by Evans and Harris⁶² who used a smaller deformation ($0.05 \leq \beta \leq 0.07$) is that the

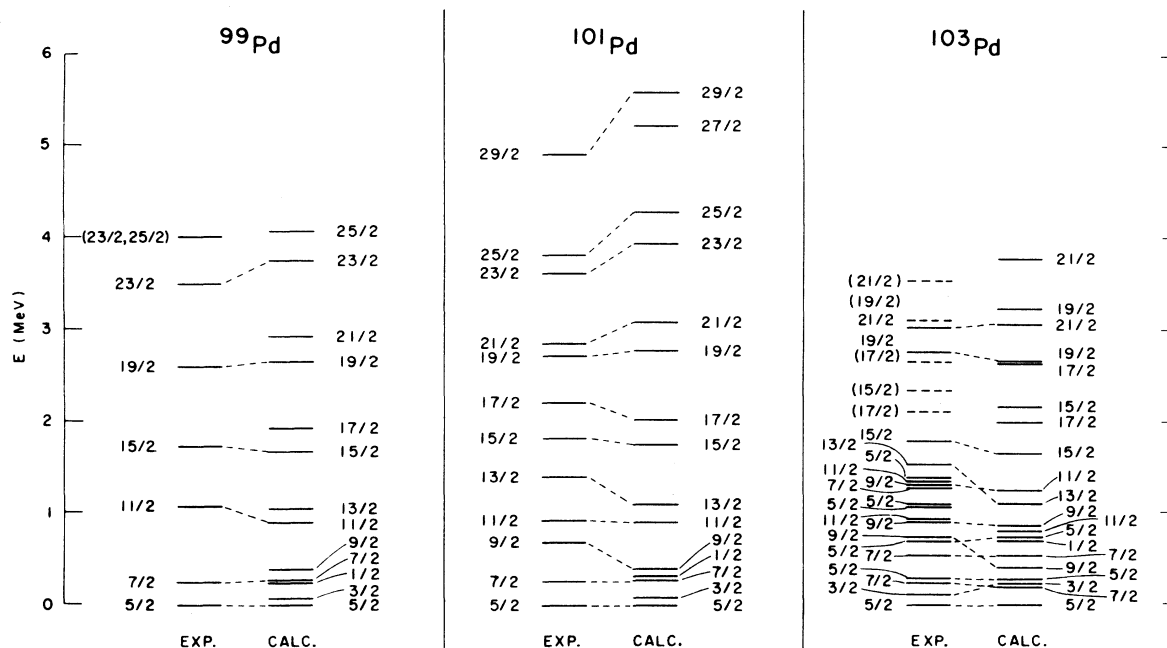


FIG. 8. Yrast positive parity level energies in $^{99,101,103}\text{Pd}$ calculated according to the rotation alignment model, as discussed in the text, compared with experimental energies. Only the yrast level calculated for each spin is plotted up to the largest spin shown except for ^{103}Pd for which eight next-to-yrast states are also shown as is dictated by the experimental evidence. The values of the elastic constant C used are (in units of 10^6 keV^3) $^{99}\text{Pd}(16)$, $^{101}\text{Pd}(19)$, and $^{103}\text{Pd}(18)$.

ground state spin of ^{105}Pd is predicted to be $J^\pi = \frac{7}{2}^+$ while the observed value is $\frac{5}{2}^+$. The latter value occurs naturally, however, in the present calculations.

A related approach of de Takacsy and Das Gupta⁶³ treats the spectra of $^{101,103,105}\text{Pd}$ by means of an axially symmetric deformed Hartree-Fock potential with pairing followed by a band-mixing calculation. Their main interest is in the odd- A Pd nuclides although they use moments of inertia and quadrupole moments deduced from the neighboring even- A Pd nuclides as input to the calculation. In this respect, their approach is the reverse of ours, in which we calculate the odd- A spectra merely for the purpose of fixing the parameters in preparation for computation of the even- A spectra. They find that the level ordering and the wave functions for $^{101,103,105}\text{Pd}$ are neither the weak-coupling nor the strong-coupling extremes.

Having performed the Nilsson diagonalization for the eleven valence neutron orbitals, we can now estimate the expectation value $\langle \hat{j}^2 \rangle$ for each quasineutron state by

$$\langle \hat{j}^2 \rangle = \sum_j C_{jk}^2 j(j+1), \quad (17)$$

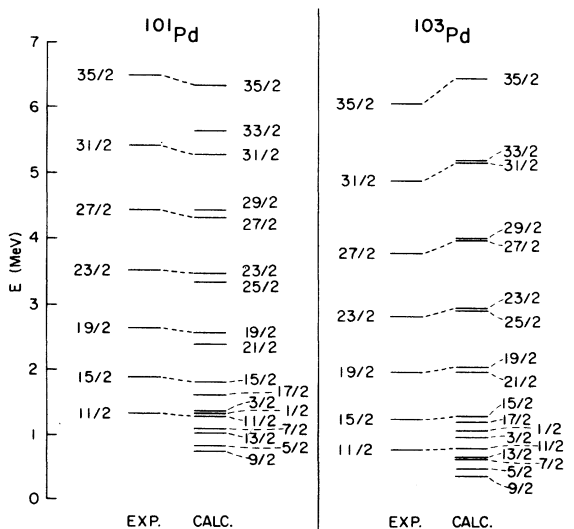


FIG. 9. Yrast negative parity level energies in ^{101}Pd and ^{103}Pd calculated according to the rotation alignment model, as discussed in the text, compared with experimental energies. The elastic constant C used for each nuclide is the same as for Fig. 8. Only the yrast level calculated for each spin is plotted up to the largest spins shown.

where the C_{jK} result from the diagonalization, and in each 3-quasineutron state by

$$\langle \hat{j}^2 \rangle = B \pm 2\Omega_1\Omega_2 \pm 2\Omega_1\Omega_3 \pm 2\Omega_2\Omega_3, \quad (18)$$

where B is the sum of three terms each of which is given by Eq. (17) evaluated for one of the three occupied orbitals, and the appropriate signs for the remaining three terms involving the projections of the three single particle angular momenta onto the nuclear symmetry axis must be used. For a given value of the elastic constant C , we may now compute the moment of inertia \mathcal{I} for each 1-quasineutron basis state or 3-quasineutron basis state by using Eq. (16) with the Coriolis decoupling term included if $K = \frac{1}{2}$,

$$\begin{aligned} & -A(J + \frac{1}{2})(-)^{J+1/2}(\frac{1}{2}/j + / - \frac{1}{2}) \\ & = -A(J + \frac{1}{2})(-)^{J+1/2} \sum_j (-)^{j+1/2}(j + \frac{1}{2})C_{j1/2}^2. \end{aligned} \quad (19)$$

Now we can evaluate the energy of each basis state by Eq. (11), including the decoupling term for $K = \frac{1}{2}$ states, and also compute the Coriolis transition matrix elements by using Eq. (12). We have used the attenuation factor $A = 0.75$ for 0- and 1-quasineutron states and the factor $A = (0.72)^2 = 0.56$ for the 2- and 3-quasineutron states. Several values of the attenuation factor are reported in the literature. For example, Stephens and Simon⁵⁶ used $A = 0.70$ while Smith and Rickey⁵⁹ used $A = 0.80$. We have also included A in the diagonal decoupling term given by Eq. (19). At this point, it is clear that we should expect to obtain different values for the nuclear moment of inertia than Smith and Rickey did⁵⁹ since we include the 3-quasineutron states while they did not.

The Coriolis diagonalization may now be performed for the odd- A Pd nuclides. The results are presented in Fig. 8 for the positive parity states and in Fig. 9 for the negative parity states. For each nuclide, we compare the calculated level energies with the empirical energies. The values of the elastic constant C used are (in units of 10^6 keV^3): $^{99}\text{Pd}(16)$, $^{101}\text{Pd}(19)$, and $^{103}\text{Pd}(18)$. For ^{99}Pd , there are six excited positive parity states known^{25,27,64} from γ -ray work and two additional states observed³⁶ from the $^{96}\text{Ru}(^{16}\text{O}, ^{13}\text{O})^{99}\text{Pd}$ reaction at 70 MeV which are expected to be positive parity states. There are not any negative parity states known in ^{99}Pd . Of the many calculated levels, we have shown only the positive parity yrast level for each spin up to $J = \frac{25}{2}$ for ^{99}Pd in Fig. 8. For ^{101}Pd , several positive and negative parity states have been found^{20,25} from γ -ray studies of high-spin states. Several additional levels below 1.3 MeV in ^{101}Pd have been found²⁶ from γ rays following the $^{103}\text{Rh}(p, 3n)$ reaction with $E_{\text{lab}} = 25\text{--}35 \text{ MeV}$. However, the spins

and parities of these levels are still under investigation. Therefore, we have omitted these levels from Fig. 8. For ^{101}Pd , we display the calculated yrast levels up to $J = \frac{29}{2}$ in Fig. 8 and up to $J = \frac{35}{2}$ in Fig. 9. An apparent defect of the calculations is that the yrast $J^\pi = \frac{9}{2}^+$ state in ^{101}Pd in Fig. 8 occurs at too low an excitation energy. This decrease in transition energies for the lowest members of a quasiparticle band is a well-known problem. For example, this problem has been discussed recently for the light barium isotopes⁶⁵ as well as for ^{104}Pd .⁶⁶ For ^{103}Pd , several positive parity states below 1.3 MeV have been populated⁶⁷ by the $^{103}\text{Rh}(p, n\gamma)^{103}\text{Pd}$ reaction, by the decay⁶⁸⁻⁷⁰ of ^{103}Ag , by the $^{104}\text{Pd}(d, t)^{103}\text{Pd}$ reaction,⁷¹ and by the $^{102}\text{Pd}(d, p)^{103}\text{Pd}$ reaction.⁷² Each of these states is displayed in Fig. 8 for ^{103}Pd if its spin and parity have been determined. In addition, we have displayed five high-spin states which have been inferred^{22,25} from the $^{94}\text{Zr}(^{12}\text{C}, 3n\gamma)^{103}\text{Pd}$ reaction but whose exact energies and spins are uncertain. However, these five states do appear to have positive parity from a consideration of the γ -ray angular distribution and linear polarization data. In Fig. 9, we have presented the seven high spin negative parity states which have been established^{22,25} in ^{103}Pd . For ^{103}Pd we have displayed in Fig. 8 the calculated positive parity levels up to $J = \frac{21}{2}$ as well as the two next-to-yrast $J^\pi = \frac{5}{2}^+$ calculated levels and the next-to-yrast calculated $J^\pi = \frac{7}{2}^+$ and $\frac{9}{2}^+$ states. For ^{103}Pd , we have also presented in Fig. 9 the calculated negative parity yrast levels up to a spin of $J = \frac{35}{2}$.

The overall correspondence of the calculated and experimental levels presented in Figs. 8 and 9 for the light odd- A Pd nuclei seems to be not bad. In particular, we can reproduce the relative depression of the $J^\pi = \frac{21}{2}^+$ and $\frac{25}{2}^+$ states in ^{101}Pd as shown in Fig. 8. Our primary interest here, however, is to calculate the 2-quasineutron spectra for ^{100}Pd and ^{102}Pd in a similar manner using the same values for the Nilsson model as are used for the odd- A Pd nuclides. The values used for the elastic constant C (in units of 10^6 keV^3) are 11 for ^{100}Pd and 14 for ^{102}Pd , and the resulting calculated levels are compared with the experimental ones in Figs. 10 and 11 for the positive and negative parity states, respectively. For both parities, we have only plotted the calculated yrast levels up to the highest spins shown. In addition, for the states in ^{102}Pd , we have presented the next-to-yrast $J^\pi = 2^+, 4^+, 6^+, 8^+, 10^+$, and 12^+ states in Fig. 10 and the next-to-yrast $J^\pi = 7^-$ and 9^- states in Fig. 11. There are several low-lying positive parity states in ^{102}Pd which are not expected to be reproduced by this 2-quasineu-

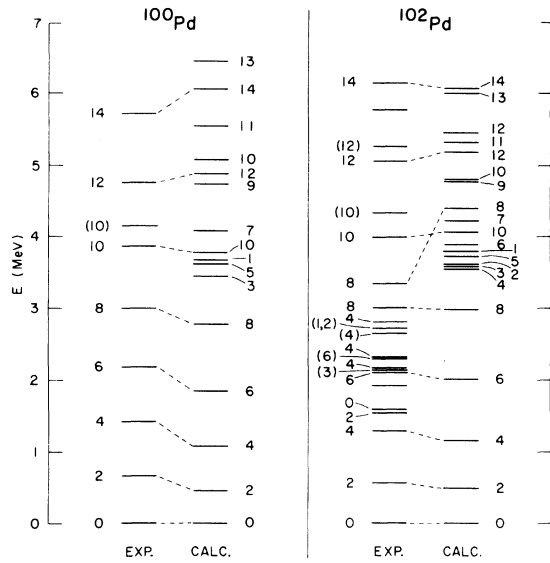


FIG. 10. Yrast positive parity level energies in ^{100}Pd and ^{102}Pd calculated according to the rotation alignment model, as discussed in the text, compared with experimental energies. The values of the elastic constant C used are (in units of 10^6keV^3) $^{100}\text{Pd}(11)$ and $^{102}\text{Pd}(14)$. Only the calculated yrast state for each spin is shown for ^{100}Pd except that the two lowest $J^\pi=10^+$ states are shown. For ^{102}Pd , six next-to-yrast states are shown in addition to the yrast ones as is dictated by experiment.

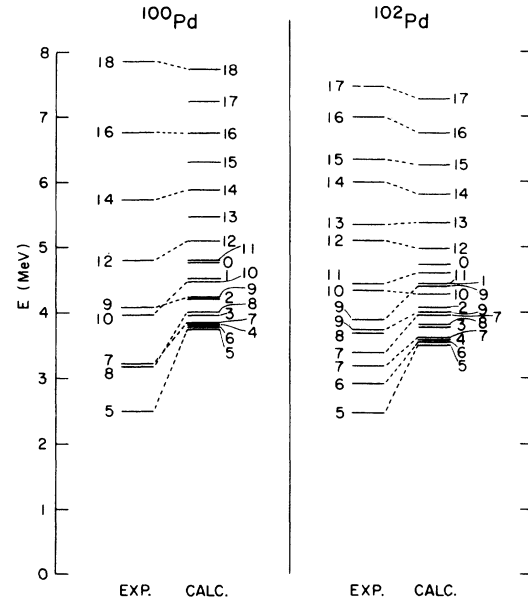


FIG. 11. Yrast negative parity energies in ^{100}Pd and ^{102}Pd calculated according to the rotation alignment model, as discussed in the text, compared with experimental energies. The elastic constant C used for each nuclide is the same as for Fig. 10. For ^{100}Pd , only the calculated yrast level is shown for each spin while for ^{102}Pd , we display the next-to-yrast $J=7, 9$ states in addition to the yrast ones as is dictated by experiment.

tron calculation. Foremost among these are the second $J^\pi=2^+$ and 0^+ states which presumably belong to the 2-phonon triplet of states arising in the vibrational model. From the calculations, however, there are not any excited $J^\pi=0^+$ states, and the next-to-lowest calculated $J^\pi=2^+$ state is at 3.6 MeV in excitation.

The positive parity calculations suggest that a 2-quasineutron band crosses below the 0-quasineutron band at the $J^\pi=14^+$ state in ^{102}Pd and at the $J^\pi=16^+$ state in ^{100}Pd . In more detail, the calculated wave function for the $J^\pi=12^+$ yrast state in ^{102}Pd is 62% 0-quasineutron (and 38% 2-quasineutron) while the $J^\pi=14^+$ state is 7% 0-quasineutron (and 93% 2-quasineutron). For ^{100}Pd , the calculated 0-quasineutron parts are 14^+ (92%), 16^+ (49%), and 18^+ (4%).

It is interesting to compare the empirical even-spin positive-parity yrast-level energies in $^{100}, ^{102}, ^{104}, ^{106}\text{Pd}$. For this purpose, we display in Fig. 12 the familiar plot of the moment of inertia \mathcal{I} for a state of spin J vs the square of the angular velocity ω of a rigid rotor, both of which are inferred from the transition energies $\Delta E(J-J-2)$ by the relations

$$\frac{2\mathcal{I}}{\hbar^2} = \frac{J(J+1) - (J-2)(J-1)}{\Delta E} = \frac{4J-2}{\Delta E} \quad (20)$$

and

$$(\hbar\omega)^2 = \left\{ \frac{\Delta E}{[J(J+1)]^{1/2} - [(J-2)(J-1)]^{1/2}} \right\}^2. \quad (21)$$

One notices immediately from Fig. 12(a) that the ground state bands of ^{104}Pd and ^{106}Pd exhibit a backbending while those of ^{102}Pd and ^{100}Pd do not. We have displayed in Fig. 12(b) the plots which result from the yrast 2-quasineutron calculations. Although a detailed comparison with the experimental plots in Fig. 12(a) does not show a spectacular resemblance, the calculations do reproduce the result that the backbend occurs at a lower spin in $^{104}, ^{106}\text{Pd}$ than for $^{100}, ^{102}\text{Pd}$. This result does not depend on the exact values of the VMI spring constant C used but rather reflects the larger number of neutron Nilsson orbitals near the Fermi level for $^{104}, ^{106}\text{Pd}$ than for $^{100}, ^{102}\text{Pd}$, thus lowering the energy of the 2-quasineutron spectrum for the former nuclides and encouraging an earlier band crossing with the 0-quasineutron band. We could, of course, adjust one or more parameters to improve the correspondence of Fig. 12(b) to Fig. 12(a) [for example, the value of

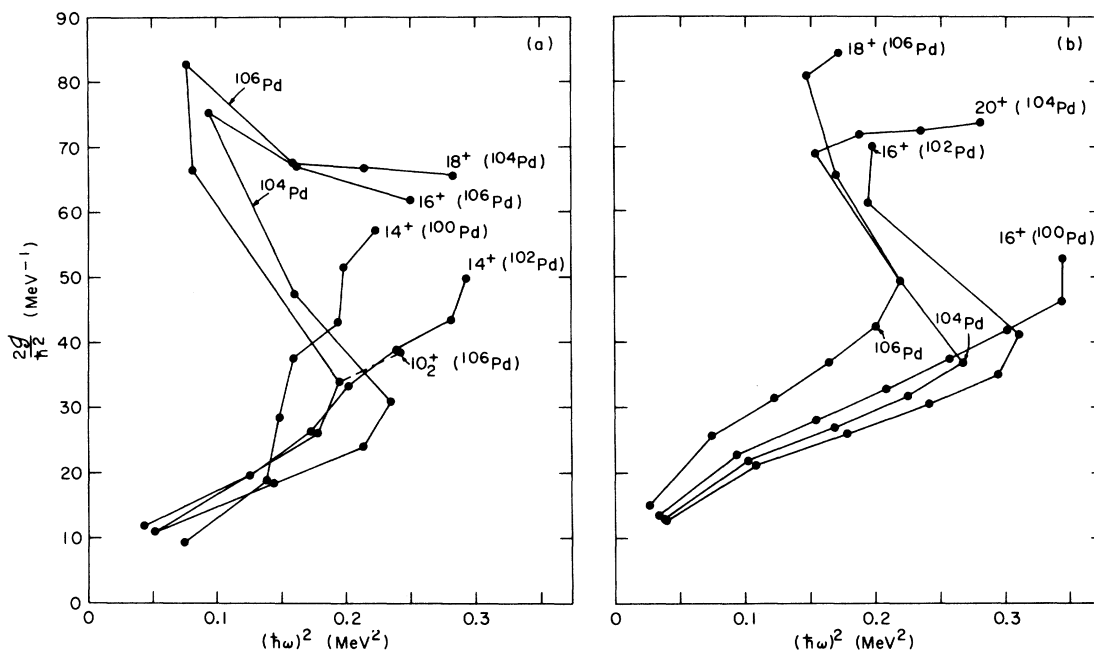


FIG. 12. A comparison of the calculated d vs ω^2 plots on the right for the $^{100,102,104,106}\text{Pd}$ ground state bands from the rotation alignment model with the experimental ones displayed on the left as discussed in the text. The values of the elastic constant C used for each nuclide are (in units of 10^6 keV 3) $^{100}\text{Pd}(11)$, $^{102}\text{Pd}(14)$, $^{104}\text{Pd}(13)$, and $^{106}\text{Pd}(8)$.

A in Eqs. (12) and (19) for the 2-quasineutron states], but we shall not do so here.

These quasiparticle calculations are satisfying in that they allow one to discuss the relation of the observed nuclear states to the motion of specific nucleons in a simple and quantitative way. The calculations reported here, however, have ignored the contribution of the valence protons to the observed spectra. The effect of the protons is reflected in a bulk manner, however, in the values of the constants κ , μ , ϵ , and Δ which are used as input. We argue, as has been done recently by Cline and Flaum⁶⁶ for ^{104}Pd , that it is in fact reasonable to consider only valence neutrons when calculating the properties of yrast states of these light-Pd nuclides since the corresponding 2-quasiproton states lie at a higher excitation energy for each spin. On the other hand, one expects that the valence protons contribute in an important way to at least some of the yrast states, and it would be interesting and worthwhile to calculate this contribution.

A comparison of the ground state band energies in all of the even-even Pd nuclei with the predictions of the VMI model (solid lines) and IBA (dashed lines) is shown in Fig. 13. The figure presents $\log_{10} R_J$ vs R_4 [the lowest curve (short dashes) indicates R_4 on the logarithmic scale, with arrows pointing to the mass numbers of the even-even Pd nuclei]. It is seen that R_4 increases

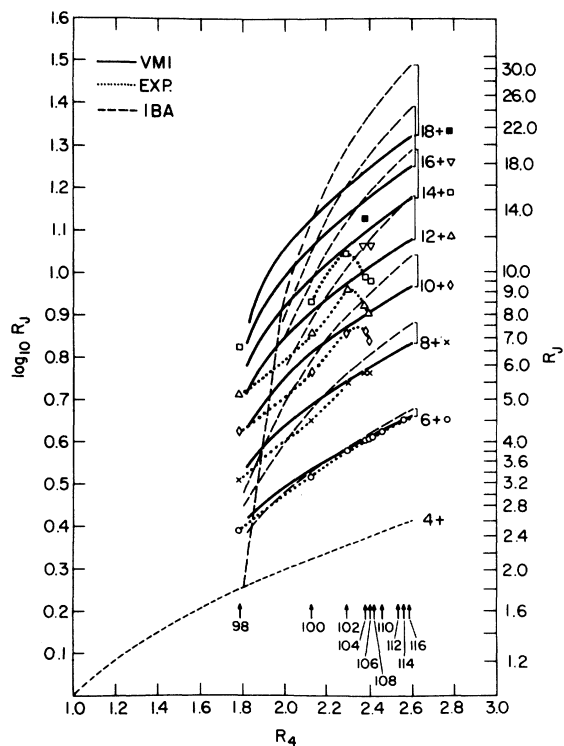


FIG. 13. The ground state band energies of the even-even Pd nuclides plotted as a function of $R_4 \equiv E_{4^+}/E_{2^+}$. The energy of each state of spin J is plotted as $R_J \equiv E_J/E_{2^+}$. Also shown are the predictions of the VMI and IBA models as discussed in the text.

with increasing neutron number. In order to guide the eye, the experimental points are connected by dotted curves. It is found that the R_6 and R_8 values for $A \geq 102$ agree very well with the VMI predictions. The points for ^{100}Pd are somewhat depressed, while those for ^{98}Pd , whose R_4 (1.786) value⁷³ lies slightly below the limit of validity (1.82) of the VMI curves, are in reasonable agreement with the extrapolated VMI curves except for the $J^\pi = 14^+$ level. The overall agreement with the IBA curves is seen to be not as good. The considerably better fit for $J^\pi = 6^+$ and 8^+ states achieved by VMI was first pointed out by Das *et al.*⁷⁴ For $J \geq 10$, only the values for ^{102}Pd agree well with VMI (but not with IBA), whereas the R_J values for ^{100}Pd are increasingly depressed. We tentatively attribute this depression to a strong four $g_{9/2}$ proton hole—four $d_{5/2}$ neutron overlap (similar to the situation in $^{132}\text{Te}_{80}$, where two $d_{5/2}$ protons appear to couple with two $h_{11/2}$ neutron holes). The R_J values for $J \geq 10$ become increasingly depressed as N increases above $N = 56$ neutrons. This behavior, which is equivalent to “backbending” above $J_c = 8$, may be ascribed to rotation aligned decoupling as discussed above. It is noteworthy that the IBA curves tend to cross each other below $R_4 = 2$, i.e., the order of the predicted states in the band is reversed—a phenomenon which contradicts observation.

The plot shown in Fig. 13 has certain advantages over the conventional \mathcal{J} vs ω^2 plots—quite apart from our particular objective, namely testing the VMI model at low R_4 values—in that it (1) permits a comparison of R_J values of a large number of nuclei at one glance, and (2) presents absolute energy ratios, which are more easily interpreted than are intervals between two subsequent states.

We note that two recent measurements have been made of the electromagnetic moments of the lowest $J^\pi = 2^+$ state in ^{102}Pd . Utilizing the inelastic excitation of ^{102}Pd by 8-MeV protons, Lange *et al.*⁵¹ have measured the reduced electric quadrupole transition probability

$$B(E2, 0^+ \rightarrow 2^+) = 0.46 \pm 0.03 e^2 b^2. \quad (22)$$

Expressed in terms of the single-proton Weisskopf estimate,⁷⁵ this is 33 Weisskopf units (W.u.). By comparison, the corresponding observed value for ^{168}Er , which is a good rotor, is 210 W.u. while for ^{120}Sn , a singly magic nuclide, the value is 12

W.u. The g factor of the lowest $J^\pi = 2^+$ state in ^{102}Pd has also recently been determined⁷⁶ to be 0.41 ± 0.04 which is near the value of $Z/A = 0.45$. Neither the $B(E2)$ nor the g factor have been measured yet for the lowest $J^\pi = 2^+$ state of ^{100}Pd . There have been two recent studies of the $^{104}\text{Pd}(p, t)^{102}\text{Pd}$ reaction^{77,78} with $E_{\text{lab}} = 21\text{--}22$ MeV. Bruzzone *et al.*⁷⁷ have located four new states from 1.9 to 2.4 MeV in excitation energy which correspond to states deduced from a study of the $^{102}\text{Pd}(p, p'\gamma)$ reaction⁵¹ with $E_{\text{lab}} = 8$ MeV. However, further work is required in order to make definitive spin assignments.

We note that the lifetime of the 1592.5-keV $J^\pi = 0^+$ state of ^{102}Pd has been recently measured.⁷⁹ Finally, the decay of ^{100}Ag to states of ^{100}Pd has been studied.⁸⁰ The energies of the $J^\pi = 2^+$ and 4^+ levels are in agreement with the present study, and in addition several new levels of low spin are reported.

To sum up, we have reported extensive new data for ^{102}Pd and ^{100}Pd . We have reported the first measurement of the γ -ray linear polarizations for ^{100}Pd and ^{102}Pd and have proposed the existence of high-spin states of ^{100}Pd . Several of the previous spin-parity assignments of ^{102}Pd have either been confirmed or called into question. The “bands” of states have been satisfactorily described by a calculation involving only a pair of neutrons decoupled from an axially symmetric core. Moreover, the transition from backbending in $^{104,106}\text{Pd}$ to the absence of backbending (at least for $J \leq 18$) in $^{100,102}\text{Pd}$ can be understood as being related to a decrease in the density of neutron orbitals close to the Fermi level.

The energies of ground state bands in the even Pd nuclei are fitted extremely well by the VMI model for $J = 6$ and 8, and moderately well up to $J = 12$, respectively, 14 for ^{98}Pd and ^{102}Pd , whereas the ground state band in ^{100}Pd is found to exhibit the same features as the bands established in other isobars of doubly magic nuclei (“pseudomagic nuclei”) [see Ref. 2(b)], namely a downward deviation of energy spacings from the VMI predictions already above $J = 4$.

We wish to thank R. C. Lee and M. McKeown as well as Dr. W. R. Kane and Dr. J. S. Lin for their help during several tandem runs. This research has been sponsored by the U. S. Department of Energy under Contract No. DE-AC02-76CH00016.

*Present address: Physics Department, State University of New York, Stony Brook, New York 11794.

†Present address: Los Alamos Scientific Laboratory, Los Alamos, New Mexico 87545.

‡Present address: Bendix Field Engineering Corp., Grand Junction, Colorado 81501.

¹M. A. J. Mariscotti, G. Scharff-Goldhaber, and B. Buck, *Phys. Rev.* **178**, 1864 (1969).

- ²(a) G. Scharff-Goldhaber and A. S. Goldhaber, *Phys. Rev. Lett.* **24**, 1349 (1970); (b) G. Scharff-Goldhaber, *J. Phys. G* **5**, L207 (1979); corrigendum, **6**, 413 (1980).
- ³G. Scharff-Goldhaber, C. Dover, and A. Goodman, *Annu. Rev. Nucl. Sci.* **26**, 239 (1976).
- ⁴G. Scharff-Goldhaber, M. McKeown, A. H. Lumpkin, and W. F. Piel, Jr., *Phys. Lett.* **44B**, 416 (1973).
- ⁵J. A. Grau, Z. W. Grabowski, F. A. Rickey, P. C. Simms, and R. M. Steffen, *Phys. Rev. Lett.* **32**, 677 (1974).
- ⁶D. C. Stromswold, Y. K. Lee, W. F. Piel, Jr., and G. Scharff-Goldhaber, *Bull. Am. Phys. Soc.* **21**, 609 (1976).
- ⁷J. Sieniawski and L. Harms-Ringdahl, Annual Report of the Stockholm Research Institute for Physics, 1970, p. 115.
- ⁸G. J. Smith, J. R. Tesmer, F. A. Rickey, P. C. Simms, and R. M. Steffen, *Bull. Am. Phys. Soc.* **17**, 466 (1972).
- ⁹W. F. Piel, Jr., A. H. Lumpkin, M. McKeown, and G. Scharff-Goldhaber, *Bull. Am. Phys. Soc.* **17**, 906 (1972).
- ¹⁰A. H. Lumpkin, W. F. Piel, Jr., M. McKeown, and G. Scharff-Goldhaber, *Bull. Am. Phys. Soc.* **17**, 906 (1972).
- ¹¹A. H. Lumpkin, W. F. Piel, Jr., G. Scharff-Goldhaber, J. S. Kim, and Y. K. Lee, *Bull. Am. Phys. Soc.* **18**, 1417 (1973).
- ¹²P. C. Simms, R. Anderson, F. A. Rickey, G. Smith, R. M. Steffen, and J. R. Tesmer, *Phys. Rev. C* **7**, 1631 (1973).
- ¹³D. C. Kocher, *Nucl. Data Sheets* **11**, 279 (1974).
- ¹⁴J. A. Grau, Z. W. Grabowski, F. A. Rickey, P. C. Simms, and G. J. Smith, *Bull. Am. Phys. Soc.* **19**, 1028 (1974).
- ¹⁵R. L. Auble, R. R. Todd, L. E. Samuelson, W. H. Kelly, and W. C. McHarris, *Nucl. Data Sheets* **19**, 1 (1976).
- ¹⁶J. A. Grau, L. E. Samuelson, F. A. Rickey, P. C. Simms, and G. J. Smith, *Phys. Rev. C* **14**, 2297 (1976).
- ¹⁷N. Sakai, T. Yamazaki, and H. Ejiri, *Nucl. Phys.* **74**, 81 (1965).
- ¹⁸S. Cochavi, M. McKeown, O. C. Kistner, and G. Scharff-Goldhaber, *J. Phys. (Paris)* **33**, No. 8-9, 102 (1972).
- ¹⁹D. C. Stromswold, D. O. Elliott, Y. K. Lee, J. A. Grau, L. E. Samuelson, F. A. Rickey, and P. C. Simms, *Phys. Rev. C* **13**, 1510 (1976).
- ²⁰P. C. Simms, F. A. Rickey, and J. R. Tesmer, *Phys. Rev. Lett.* **30**, 710 (1973).
- ²¹F. A. Rickey and P. C. Simms, *Phys. Rev. Lett.* **31**, 404 (1973).
- ²²J. A. Grau, F. A. Rickey, G. J. Smith, P. C. Simms, and J. R. Tesmer, *Nucl. Phys.* **A229**, 346 (1974).
- ²³P. C. Simms, G. J. Smith, F. A. Rickey, J. A. Grau, J. R. Tesmer, and R. M. Steffen, *Phys. Rev. C* **9**, 684 (1974).
- ²⁴A. H. Lumpkin, L. H. Harwood, L. A. Parks, and J. D. Fox, *Phys. Rev. C* **17**, 376 (1978).
- ²⁵J. S. Kim, Y. K. Lee, K. A. Hardy, P. C. Simms, J. A. Grau, G. J. Smith, and F. A. Rickey, *Phys. Rev. C* **12**, 499 (1975).
- ²⁶H. A. Smith, Jr., I. Aguirre, P. P. Singh, M. E. Sadler, A. Nadasen, and L. A. Beach, *Bull. Am. Phys. Soc.* **21**, 995 (1976).
- ²⁷W. F. Piel, Jr., and G. Scharff-Goldhaber, *Phys. Rev. C* **15**, 287 (1977).
- ²⁸G. Scharff-Goldhaber and J. Weneser, *Phys. Rev.* **98**, 212 (1955).
- ²⁹F. Iachello, *Proceedings of the International Conference on Nuclear Structure and Spectroscopy, Amsterdam, 1974*, edited by H. P. Blok and A. E. L. Dieperink (Scholar's Press, Amsterdam, 1974) Vol. 2, pp. 163-181.
- ³⁰F. Iachello and A. Arima, *Phys. Lett.* **53B**, 309 (1974).
- ³¹H. Feshbach and F. Iachello, *Ann. Phys. (N. Y.)* **84**, 211 (1974).
- ³²A. Arima and F. Iachello, *Phys. Lett.* **57B**, 39 (1975).
- ³³K. S. Krane, R. M. Steffen, and R. M. Wheeler, *Nucl. Data, Sect. A11*, 351 (1973).
- ³⁴K. A. Hardy, A. Lumpkin, Y. K. Lee, G. E. Owen, and R. Shnidman, *Rev. Sci. Instrum.* **42**, 482 (1971).
- ³⁵A. H. Lumpkin, A. W. Sunyar, K. A. Hardy, and Y. K. Lee, *Phys. Rev. C* **9**, 258 (1974).
- ³⁶C. E. Thorn, P. D. Bond, M. J. LeVine, W. F. Piel, Jr., and A. Gallmann, *Bull. Am. Phys. Soc.* **23**, 72 (1978).
- ³⁷T. Yamazaki, *Nucl. Data Sect. A3*, 1 (1967).
- ³⁸D. Strominger, J. M. Hollander, and G. T. Seaborg, *Rev. Mod. Phys.* **30**, 585 (1958).
- ³⁹O. Ames, A. M. Bernstein, M. H. Brennan, R. A. Haberstroh, and D. R. Hamilton, *Phys. Rev.* **118**, 1599 (1960).
- ⁴⁰P. Charoenkwan and J. R. Richardson, *Bull. Am. Phys. Soc.* **8**, 595 (1963).
- ⁴¹P. Charoenkwan and J. R. Richardson, *Nucl. Phys.* **A94**, 417 (1967).
- ⁴²F. D. S. Butement and M. Y. Mirza, *J. Inorg. Nucl. Chem.* **28**, 303 (1966).
- ⁴³H. Bakhru, R. I. Morse, and I. L. Preiss, *Nucl. Phys.* **A100**, 145 (1967).
- ⁴⁴B. S. Dzhelepov, L. K. Peker, and V. M. Sigalov, Report No. 076 of Physics and Technical Institute, Leningrad, 1968.
- ⁴⁵B. Greenebaum, A. D. Jackson, Jr., and R. A. Naumann, *Nucl. Phys.* **A106**, 193 (1968).
- ⁴⁶J. Liptak, J. Vrzal, E. P. Grigoriev, G. S. Katykhin, and J. Urbanec, *Czech. J. Phys.* **B19**, 1127 (1969).
- ⁴⁷E. Beck, *Proceedings of the International Conference on the Properties of Nuclei Far from the Regions of Beta-Stability, Leysin, Switzerland, 1970* [CERN Report No. 70-30, 1970 (unpublished)], p. 353.
- ⁴⁸D. J. Hnatowich, F. Munnich, and A. Kjelberg, *Nucl. Phys.* **A178**, 111 (1971).
- ⁴⁹J. van Klinken, S. J. Feenstra, K. Wisshak, and H. Faust, *Nucl. Instrum. Methods* **130**, 427 (1975).
- ⁵⁰S. J. Feenstra, J. M. Galema, and J. van Klinken, KVI Annual Report, 1975.
- ⁵¹J. Lange, A. T. Kandil, J. Neuber, C. D. Uhlhorn, H. von Buttlar, and A. Bockisch, *Nucl. Phys.* **A292**, 301 (1977); A. T. Kandil, *J. Inorg. and Nucl. Chem.* **40**, 1853 (1978).
- ⁵²T. Inamura, A. Hashizume, T. Katou, and Y. Tendow, *J. Phys. Soc. Jpn.* **30**, 884 (1971).
- ⁵³H. Ejiri, M. Ishihara, M. Sakai, K. Katori, and T. Inamura, *J. Phys. Soc. Jpn.* **24**, 1189 (1968).

- ⁵⁴M. J. A. de Voigt, Z. Sujkowski, D. Chmielewska, J. F. W. Jansen, J. van Klinken, and S. J. Feenstra, *Phys. Lett.* **59B**, 137 (1975); M. J. A. de Voigt, J. F. W. Jansen, F. Bruining, and Z. Sujkowski, *Nucl. Phys.* **A270**, 141 (1976).
- ⁵⁵H. H. Hsu, S. A. Williams, F. K. Wohn, and F. J. Margetan, *Phys. Rev. C* **16**, 1626 (1977).
- ⁵⁶F. S. Stephens and R. S. Simon, *Nucl. Phys.* **A183**, 257 (1972).
- ⁵⁷F. S. Stephens, P. Kleinheinz, R. K. Sheline, and R. S. Simon, *Nucl. Phys.* **A222**, 235 (1974).
- ⁵⁸W. F. Piel, Jr., *Bull. Am. Phys. Soc.* **18**, 1404 (1973).
- ⁵⁹H. A. Smith, Jr., and F. A. Rickey, *Phys. Rev. C* **14**, 1946 (1976).
- ⁶⁰S. G. Nilsson, *K. Dan Vidensk. Selsk. Mat. Fys. Medd.* **29**, No. 16 (1955).
- ⁶¹B. Nilsson, *Nucl. Phys.* **A129**, 445 (1969).
- ⁶²P. J. Evans and S. M. Harris, *Phys. Rev. C* **17**, 1210 (1978).
- ⁶³N. de Takacsy and S. Das Gupta, *Nucl. Phys.* **A263**, 237 (1976).
- ⁶⁴D. R. Doty, J. R. Richardson, and J. W. Sunier, *Nucl. Phys.* **A103**, 417 (1967).
- ⁶⁵C. Flaum, D. Cline, A. W. Sunyar, O. C. Kistner, Y. K. Lee, and J. S. Kim, *Nucl. Phys.* **A264**, 291 (1976).
- ⁶⁶C. Flaum and D. Cline, *Phys. Rev. C* **14**, 1224 (1976).
- ⁶⁷D. L. Matthews, M. Koike, and C. F. Moore, *Nucl. Phys.* **A177**, 577 (1971).
- ⁶⁸A. P. Patro and B. Basu, *Phys. Rev.* **127**, 1258 (1962).
- ⁶⁹A. D. Jackson, Jr., J. S. Evans, R. A. Naumann, and J. D. McCullen, *Phys. Rev.* **151**, 956 (1966).
- ⁷⁰H. Bakhru, R. I. Morse, and I. L. Preiss, *Can. J. Phys.* **47**, 419 (1969).
- ⁷¹B. Cujec, *Phys. Rev.* **131**, 735 (1963).
- ⁷²S. Hayakawa, Ph.D. thesis, Florida State University (1966).
- ⁷³W. F. Piel, Jr. and G. Scharff-Goldhaber, *Bull. Am. Phys. Soc.* **23**, 555 (1978).
- ⁷⁴T. K. Das, R. K. Dreizler, and A. Klein, *Phys. Rev. C* **2**, 632 (1970); A. Klein, *Phys. Lett.* **93B**, 1 (1980).
- ⁷⁵J. M. Blatt and V. F. Weisskopf, *Theoretical Nuclear Physics* (Wiley, New York, 1952), p. 627.
- ⁷⁶J. M. Brennan, M. Hass, and N. Benczer-Koller, *Bull. Am. Phys. Soc.* **23**, 555 (1978); J. M. Brennan, M. Hass, N. K. B. Shu, and N. Benczer-Koller, *Phys. Rev. C* **21**, 574 (1980).
- ⁷⁷C. Bruzzone, D. Rehbein, S. Kubono, D. Palmer, and N. Hintz, 1977 Annual Report, University of Minnesota, p. 118.
- ⁷⁸K. Yagi, S. Kumori, Y. Aoki, K. Nagano, Y. Tagishi, and Y. Toba, University of Tsukuba, Japan, Report No. UTTAC-9, 1978.
- ⁷⁹K. Cornelis, G. Lhersonneau, M. Huyse, D. Vandeplasche, and J. Verplancke, *Z. Phys. A* **292**, 403 (1979).
- ⁸⁰H. I. Hayakawa, I. Hyman, and J. K. P. Lee, *Phys. Rev. C* **22**, 247 (1980).